



HAL
open science

Sub-optimal recursively feasible Linear Parameter-Varying predictive algorithm for semi-active suspension control

Marcelo Menezes Morato, Julio E Normey-Rico, Olivier Sename

► **To cite this version:**

Marcelo Menezes Morato, Julio E Normey-Rico, Olivier Sename. Sub-optimal recursively feasible Linear Parameter-Varying predictive algorithm for semi-active suspension control. *IET Control Theory and Applications*, 2020, 14 (18), pp.2764-2775. 10.1049/iet-cta.2020.0592 . hal-02924234

HAL Id: hal-02924234

<https://hal.science/hal-02924234>

Submitted on 1 Sep 2020

HAL is a multi-disciplinary open access archive for the deposit and dissemination of scientific research documents, whether they are published or not. The documents may come from teaching and research institutions in France or abroad, or from public or private research centers.

L'archive ouverte pluridisciplinaire **HAL**, est destinée au dépôt et à la diffusion de documents scientifiques de niveau recherche, publiés ou non, émanant des établissements d'enseignement et de recherche français ou étrangers, des laboratoires publics ou privés.

A Sub-Optimal Recursively Feasible Linear Parameter Varying Predictive Algorithm for Semi-Active Suspension Control

Marcelo Menezes Morato^{a,b}, Julio E. Normey-Rico^a, Olivier Sename^b

^a*Departamento de Automação e Sistemas (DAS), Universidade Federal de Santa Catarina, Florianópolis, Brazil*

^b*Université Grenoble Alpes, CNRS, GIPSA-lab, Grenoble, France*

Abstract

This paper proposed a control algorithm to enhance the comfort of passengers in a vehicle equipped with Semi-Active Suspension systems, manipulating the force delivered by the Semi-Active damper. For this goal, the vertical dynamics of the car are represented through a quasi-Linear Parameter Varying (qLPV) model. Then, the algorithm resides in solving a set-constrained Model Predictive Control (MPC) problem, embedding a comfort performance index to the MPC optimization function. The sub-optimality of this algorithm resides in the fact that the MPC is synthesized considering a frozen guess for the evolution of the qLPV scheduling parameters along the prediction horizon. Assuming bounds on the variation rates of the qLPV scheduling parameters, the method enables a replacement of the original complex nonlinear LPV MPC optimization by a much simpler Quadratic Program (QP). This QP includes a Lyapunov-decreasing stage cost and embeds set-based terminal ingredients, which guarantee that the domain of attraction of the controller is enlarged and that recursive feasibility can be maintained despite the non-exact model scheduling (and suboptimality). The control structure is tested and compared to other optimal control approaches, such as a clipped Linear Quadratic Regulator. The paper ends with successful realistic nonlinear simulations of a 1/5-scaled car with Electro-Rheological suspensions, which illustrate the overall good operation and behaviour achieved with the proposed regulation algorithm. With the proposed method, the comfort of the passengers is substantially improved.

1. Introduction

1.1. Semi-Active Suspension Systems

The suspension system of a car is the mechanism that acts to enhance the driving performance with respect to roll handling and passenger comfort. Semi-Active (SA) suspensions are today the standard component in many state-of-the-art high-range cars and a good deal of academic and industrial research works have been focused on their control. SA suspensions are well-performing, energy-efficient and altogether less expensive than Active ones, for instance. Further context and details can be found in [1, 2].

Many design algorithms have been proposed for the SA suspension control problem. The main issue is how to handle the dissipativity constraints of the SA dampers while ensuring good performances. Papers [3, 4] detail some the available methods proposed for this goal (see references therein). Some of the most modern techniques have been tested, such as clipped optimal LQRs in [5], H_∞ techniques [6], Linear Parameter Varying (LPV) approaches [7], and nonlinear methods, such as backstepping [8].

1.2. Predictive Control

Although all these approaches achieve good performances, a more natural framework for optimal control of constrained process is Model Predictive Control (MPC) [9]. MPC is indisputably a very well established

Email addresses: marcelomnzm@gmail.com (Marcelo Menezes Morato), julio.normey@ufsc.br (Julio E. Normey-Rico), olivier.sename@gipsa-lab.fr (Olivier Sename)

16 feedback control technique, with success in many industrial applications. This method allows to explicitly
17 consider input and state constraints in the design process and solves the constrained optimization problem
18 at each sampling instant to determine the control policy. For its formulation, MPC requires a fidel process
19 model, so that the future output predictions can be expressed with respect to current input and state values.

20 The original MPC framework was attached to the idea of processes with linear time-invariant (LTI)
21 models. This condition is inherently violated for almost all plants with a wide range of operating conditions,
22 which require nonlinear forecasting models. Therefore, MPC has been progressively extended to embed
23 nonlinear model predictions (NMPC) as discusses [10], but this kind of nonlinear design is not trivial and
24 has increased numerical complexity, suffering from issues related to their high complexity when sought to
25 run in real-time. It is a known fact that the computational requirements of MPC may be excessive in many
26 situations, since the optimization problem which has to be solved online, at each sampling instant.

27 SA suspension control consists, basically, in varying the damping coefficient, which implies in variations
28 on the delivered force. The dissipativity constraints of the damper are, thus, input constraints, and this kind
29 of problem falls into a saturation paradigm which is elegantly dealt with by MPC. Some papers have indeed
30 employed MPC for SA suspension control. In this paper, the focus is given to reduced-order car frameworks
31 (such as the quarter-car or de half-car models), which decouple the vertical dynamics by vehicle corner or
32 side to reduce the complexity of the yielded MPC algorithm (quarter-car models reduce number of states by
33 a third, roughly, with respect to full-car models). The idea of solving the control problem for each vehicle
34 corner (or side) is appealing when passenger comfort is the main concern, because the coupling and load
35 transfer distribution between corners can be neglected as their influence upon comfort is small, as discusses
36 [11]. The following SA suspension control papers that apply MPC reduced-order models are recalled:

- 37 • A methodology for performance evaluation of SA suspensions under optimal control algorithm (MPC
38 included) is presented in [12]. The method enables to evaluate passenger comfort and vehicle handling
39 w.r.t. differente road profiles;
- 40 • Both [13] and [14] proposed clipped (saturated) versions of optimal control. Since the clipping action
41 is not embedded into the optimization procedure due to nonlinearities that aimed to be avoided, the
42 results do not represent optimality;
- 43 • An MPC algorithm is formulated for an LPV quarter-car model in [15]. Anyhow, there are no as-
44 sessments on feasibility guarantees of the proposed tool, which simply considers as if the scheduling
45 parameters were fixed along the horizon, for the MPC computation;
- 46 • In [16], the predictive controller is synthesized for a half-car model with some experimental validation,
47 but the effect of the road disturbances is neglected. The achieved results are interesting and the control
48 policy is implemented within 10 ms.

49 *Remark 1.* With respect to the Author's previous works, in [11, 17] fast MPC algorithms were developed
50 considering full car models. The inputed nonlinearity and the dissipativity constraints are adapted using a
51 pre-filter, which makes the model, from the MPC viewpoint, LTI. This pre-filtering technique, for practical
52 purposes, may cause implementation distress, given that a bilinear term $\dot{z}_{def}(k)u(k)$ is converted into a
53 linear term $\dot{z}_{def}(k)u_{nom} + u_f(k)$ by this pre-filter, which means that a division by $\dot{z}_{def}(k)$ is necessary
54 and, for situations when this velocity term approaches zero, the pre-filtering must be adapted. Note that
55 near-zero piston velocity situations are very common in SA suspensions (constant straight road profile, for
56 instance). Moreover, the optimization procedure is adapted using some heuristics (Infeasible Start Newton
57 Method, Primal-Barrier term) so that the MPC can run within 5 ms, which also implies in sub-optimal
58 results. Finally, these two papers lack analysis in the recursive feasibility property of the algorithm, which
59 is required when dealing with multiple road profiles.

60 1.3. Main Motivation

61 It seems that the majority of predictive control algorithms applied for automotive SA suspension systems
62 that are able to run in real-time achieve sub-optimal results. This fact does not mean that they do not

63 enhance the performances of these systems w.r.t. other control frameworks. Indeed, most papers show
 64 good performance enhancements. Nonetheless, up to the Author’s best knowledge, no paper has presented
 65 recursive feasibility assessments on these MPC algorithms, which are very necessary to ensure that the
 66 control method can run despite the model simplifications. Therefore, the main motivation of this paper is
 67 to present a predictive control algorithm for vehicular SA suspensions that embed the recursive feasibility
 68 property.

69 The majority of reduced-order models for SA suspensions that handle the dissipativity constraints of the
 70 dampers have nonlinear characteristics. The pre-filtering method, as discussed in Remark 1 is not such a
 71 good option concerning real implementation.

72 Today, generalized formulations of NMPC are available to deal with such models, but, as highlighted,
 73 they are generally not able to run fast enough. Recently, the use of LPV models [18, 19] has been brought
 74 to focus to tackle and facilitate the control of nonlinear processes; such models are also nonlinear, but are
 75 “coordinated” by bounded, known scheduling parameters ρ . Due to these parameters, LPV models are much
 76 simpler to represent than full nonlinear ones, being quite similar to the LTI framework; for this reason, LPV
 77 models have become very popular for NMPC control purposes [20]. MPC design based on LPV models has
 78 formally been studied since the beginning of the 00’s, but this field is still open for investigation (in Section
 79 3, a brief overview of the LPV MPC state-of-the-art is presented).

80 In fact, feasible LPV MPC algorithms with Quadratic Programming (QP) level complexity are rather
 81 scarce. The available methods either rely on heavy offline procedures or are too conservative (solving a
 82 robust problem with respect to all possible trajectories for ρ). Moreover, the sub-optimal methods that are
 83 not too conservative have a lack of recursive feasibility holds.

84 1.4. Contributions

85 Many nonlinear processes can be described within an LPV formalism, as long as linear differential
 86 inclusion is respected [21], and so is the case of SA suspension systems.

87 Motivated by the reasons discussed above, this paper seeks the development of a predictive control
 88 policy for SA suspensions that enhances the comfort of the onboard passengers. The proposed algorithm
 89 is adapted from [22], is based on an LPV model of the suspension and considers bounded rates of the
 90 scheduling parameters, as suggested by [20], and evaluating its recursive feasibility holds. The new method
 91 simplifies the computation of the control-invariant sets which are computed using a worst-case scenario for
 92 the evolution of the parameters, resulting in a practically implementable version.

93 Hence, the main contributions of this paper are listed below:

- 94 • A control-oriented LPV model for vehicular SA suspension systems is proposed (Section 2). This model
 95 is corroborated with respect to the comfort performance indexes proposed by [12]. The dissipativity
 96 properties of the SA dampers are embedded to the model as input constraints.
- 97 • Using a frozen guess for the future evolution of the scheduling parameters, provided at each sampling
 98 instant k , the novel qLPV MPC algorithm is proposed (Section 4). This algorithm is based on a
 99 standard QP coupled to contractive terminal set constraints and a Lyapunov-decreasing terminal
 100 stage cost. The terminal set is computed using thanks to the bounds on the scheduling parameter
 101 variations.
- 102 • Considering a high-fidelity nonlinear model for a real vehicle testbed with four Electro-Rheological SA
 103 dampers, numerical simulations of the proposed algorithms are presented (Section 5). The proposed
 104 method is compared with respect to other algorithms from the literature (as a clipped LQR). The
 105 results demonstrate the effectiveness of the proposed tool to enhance the comfort of the onboard
 106 passengers; performance indexes from [12] are used for evaluation.

107 Note that a brief overview of the available LPV MPC methods is presented in Section 3. Moreover, this
 108 Section presents the standard MPC design or the case of systems described via qLPV models, making it
 109 evident how the evolution of ρ becomes a computational issue, since: *i*) it is (*a priori*) unknown; and *ii*) it
 110 transforms the optimization procedure into a nonlinear one. It is also shown how the nonlinear optimization

111 can be converted into a QP by using a frozen evolution guess for the future values of ρ . General conclusions
 112 of the paper and a debate on the achieved results are drawn in Section 6.

113 *Remark 2.* Let the difference between LPV and qLPV models be cleared: the scheduling parameters in the
 114 LPV case are exogenous, unknown and must be pre-specified, while in the qLPV case they are available dur-
 115 ing the prediction horizon computations from a (possibly nonlinear) map of states and inputs $f_\rho(x(k), u(k))$.
 116 A direct consequence of these issues is that, considering MPC design, stability is typically dealt with in a
 117 robust worst-case level for the LPV case, while rendered as nonlinear programs for the qLPV scenario.
 118 This work is mainly concerned with the latter class of systems, addressing the issue with a sub-optimal QP
 119 method.

120 2. A Control-Oriented qLPV Corner Model for Vehicle Vertical Dynamics

121 In this paper, a SA suspension control system is developed for a vehicle with 4 Electro-Rheological (SA)
 122 dampers. The control system is composed of four MPC algorithms, one concerned with the performances of
 123 each vehicle corner. Indeed, a qLPV representation is provided in this Section for each corner of the vehicle.
 124 This qLPV model enables to express the nonlinear dissipativity constraints of the dampers into linear input
 125 constraints.

126 The control-oriented qLPV corner model is adapted from [23]; it serves for design and analysis purposes.
 127 The model involves the vertical dynamics of the vehicle, at each corner, considering the chassis dynamics
 128 (z_s) and the displacements of the wheel link (z_{us}), which are meddled by the road profile disturbances (z_r).
 129 Figure 1 shows a schematic representation of a vehicle corner. This 2DOF model is governed by the following
 130 laws:

$$\begin{cases} m_s \ddot{z}_s(t) &= -F_s(t) - F_d(t), \\ m_{us} \ddot{z}_{us}(t) &= F_s(t) + F_d(t) - F_t(t), \end{cases} \quad (1)$$

131 where $F_s(t)$, $F_d(t)$ and $F_t(t)$ represent, respectively, the force delivered by spring, by the (controlled) damper
 132 and by the tire.

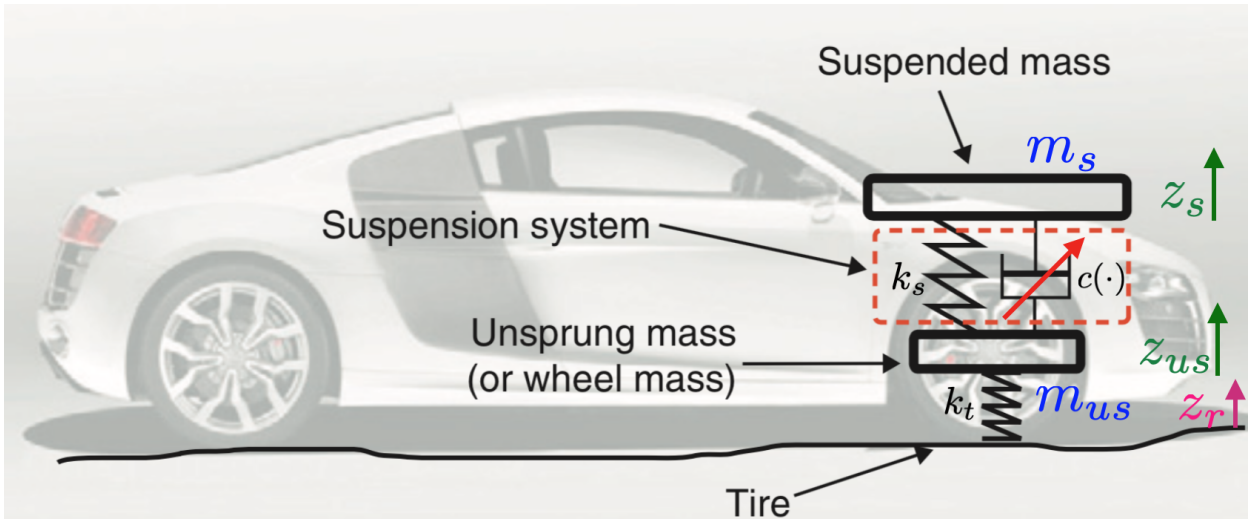


Figure 1: Vehicle Corner with Semi-Active Suspension System

133 These forces are further detailed: the spring force and the tire force are given as respectively proportional
 134 to the suspension deflection ($z_{def} = z_s - z_{us}$) and the wheel deflection, as follows:

$$F_s(t) = k_s z_{def}(t), \quad (2)$$

$$F_t(t) = k_t (z_{us}(t) - z_r(t)), \quad (3)$$

135 being k_s and k_t the stiffnesses of the spring and the tire, respectively. Finally, the damper force is given as
 136 follows:

$$F_d(t) = k_0 z_{def}(t) + c(\cdot) \dot{z}_{def}(t), \quad (4)$$

137 where $c(\cdot)$ is the damping coefficient which is the control input to the SA system.

138 The dissipativity constraints of the SA damper are set upon $F_d(t)$, which must always lie within a
 139 feasibility set whose form is roughly illustrated in Figure 2. This dissipativity set has a hysteresis-like
 140 behaviour and can be represented by the following inequalities:

$$\bar{F}_d \leq F_d(t) \leq \bar{F}_d, \quad (5)$$

$$0 \leq \underline{c} \leq c(\cdot) \leq \bar{c}. \quad (6)$$

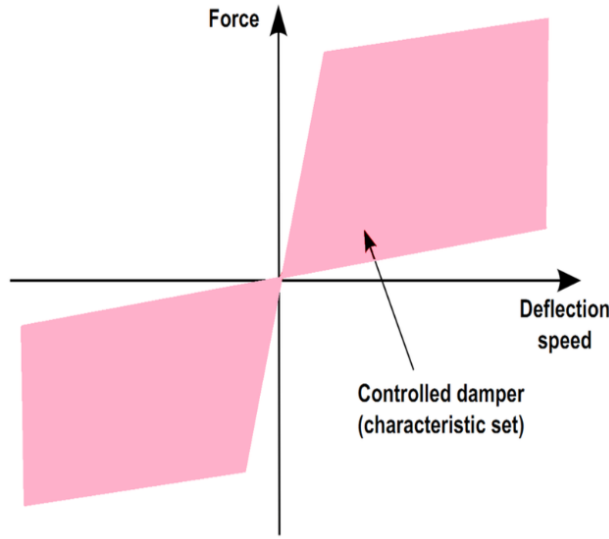


Figure 2: Semi-Active Damper: Feasible Force Region

141 To incorporate these inequalities into a simpler framework for design purposes, the damper force is
 142 traced as the static nonlinear map, as suggests [24], which can be used for both Magneto-rheological or
 143 Electro-rheological dampers (the technologies present in majority of SA suspensions), as follows:

$$F_d(t) = k_0 z_{def}(t) + c_0 \dot{z}_{def}(t) + \rho(t) u(t), \quad (7)$$

where the scheduling parameter

$$\rho(t) = f_c \tanh(k_1 z_{def}(t) + c_1 \dot{z}_{def}(t))$$

144 directly embeds the hysteresis-like behaviour of the SA damper. Parameters k_0 and c_0 denote the nominal
 145 stiffness and damping coefficient of the SA damper; moreover, $u(t)$ denotes the duty cycle of a PWM signal
 146 that regulates the voltage input which provides the electrical field upon the damper. This electric field varies
 147 the viscosity of the MR/ER fluid. In practice, it is this PWM signal $u(t)$ that acts as the control input to
 148 the suspension application. Then, the dissipativity constraints are expressed as simple input constraints:
 149 $0 < u(t) < 1$.

150 The suspension deflection velocity variable $\dot{z}_{def}(t)$ is bounded, due to physical limits (converted as
 151 constraints on the system variables), and can be measured or, a least, accurately estimated. Therefore, $\rho(t)$
 152 is also known and bounded at each instant, serving as the scheduling variable for the qLPV model.

Then, the state-space representation of the qLPV consists in re-writing Eq. (1) with

$$x(t) = [z_s(t), \dot{z}_s(t), z_{us}(t), \dot{z}_{us}(t)]^T$$

as system states:

$$\begin{aligned} \dot{x}(t) &= A_c x(t) + B_{c_1}(\rho(t))u(t) + B_{c_2} z_r(t) \\ y(t) &= C_c x(t) + D_{c_1}(\rho(t))u(t) + D_{c_2} z_r(t) \end{aligned} \quad (8)$$

Remark 3. In this paper, as done in many practical applications, the measured outputs of the SA suspension system are acceleration variables. These accelerations can be measured using accelerometers/inertial units, that are widely present in top-cars. These sensors are the ones used for the control of vertical dynamic behaviours. No additional sensors are needed, but the on-board ones [23].

Remark 4. As displayed in many papers from the literature [25, 23], with experimental validation included, observers can be used, using acceleration variables, to estimate the states of SA suspensions, considering corner models. Therefore, in the sequel, it is assumed that the system states are estimated by some observer scheme and available, in real-time, to the control system.

For the reasons discussed above, the two acceleration variables from Eq. (1) are measured, i.e. $y(t) = [\ddot{z}_s(t), \ddot{z}_{us}(t)]^T$. Therefore, the matrices in Eq. (8) are the following:

$$\begin{aligned} A_c &= \begin{bmatrix} 0 & 1 & 0 & 0 \\ \frac{-(k_s+k_0)}{m_s} & \frac{-c_0}{m_s} & \frac{(k_s+k_0)}{m_s} & \frac{c_0}{m_s} \\ 0 & 0 & 0 & 1 \\ \frac{(k_s+k_0)}{m_{us}} & \frac{c_0}{m_{us}} & \frac{-(k_s+k_0+k_t)}{m_{us}} & \frac{-c_0}{m_{us}} \end{bmatrix}, \\ B_{c_1}(\rho(t)) &= \begin{bmatrix} 0 & \frac{-\rho}{m_s} & 0 & \frac{\rho}{m_{us}} \end{bmatrix}^T, \\ B_{c_2} &= \begin{bmatrix} 0 & 0 & 0 & \frac{k_t}{m_{us}} \end{bmatrix}^T, \\ C_c &= \begin{bmatrix} \frac{-(k_s+k_0)}{m_s} & \frac{-c_0}{m_s} & \frac{(k_s+k_0)}{m_s} & \frac{c_0}{m_s} \\ \frac{(k_s+k_0)}{m_{us}} & \frac{c_0}{m_{us}} & \frac{-(k_s+k_0+k_t)}{m_{us}} & \frac{-c_0}{m_{us}} \end{bmatrix}, \\ D_{c_1}(\rho(t)) &= \begin{bmatrix} \frac{-\rho}{m_s} & \frac{\rho}{m_{us}} \end{bmatrix}^T, \\ D_{c_2} &= \begin{bmatrix} 0 & \frac{k_t}{m_{us}} \end{bmatrix}^T. \end{aligned}$$

Remark 5. Due to physical limits of the SA suspension, constraints are also set upon the system states, considering $n_x = 4$ and $n_u = 1$:

$$x(t) \in \mathcal{X} := \{x_j \in \mathbb{R}^{n_x} \mid \underline{x}_j \leq x_j \leq \bar{x}_j\}. \quad (9)$$

The input constraints are:

$$u(t) \in \mathcal{U} := \{u \in \mathbb{R}^{n_u} \mid 0 < u \leq 1\}. \quad (10)$$

Conversely, the dissipativity constraints are:

$$F_d(t) \in \mathcal{D} := \{F_d \in \mathbb{R}^{n_u} \mid \underline{F}_d \leq F_d \leq \bar{F}_d\}, \quad (11)$$

which are always respected if $x \in \mathcal{X}$ and $u \in \mathcal{U}$.

2.1. Performances Indexes

As discussed by the references of automotive Semi-Active suspensions, the main objective of these systems is to isolate the vehicle body from the disturbances implied by the road through which the car is driven [2]. At the same time, the comfort of the onboard passengers must be enhances.

173 These two objectives (vehicle body isolation and passenger comfort) are physically conflicting. Stiff/high
 174 damping enhances passenger comfort, while smooth/low damping enables easier road holding, see [12].
 175 Anyhow, since this paper consider a quarter-car vehicle corner model, it is assumed that a central controller
 176 for the braking system will be concerned with the first objective, of isolating the vehicle body from road
 177 trepidations, reducing the roll angle of the car and enhancing handling concerns. This kind of controller is
 178 seen in different papers, e.g. [26, 27].

179 Therefore, the corner controllers are concerned with passenger comfort performances. As proposed in
 180 [12], a simple methodology to evaluate the comfort of the onboard passengers is to analyse the car's center-of-
 181 gravity (COG) acceleration. At each corner, this analysis is reduced to the acceleration of the sprung-mass
 182 (chassis body), given by $\ddot{z}_s(t)$.

183 The vertical chassis acceleration $\ddot{z}_s(t)$ response to the road disturbances $z_r(t)$ can be evaluated between 0
 184 and 20 Hz for comfort specifications, as discussed in [28]. The two criteria from [12] to evaluate the comfort
 185 of the passengers, within these frequencial bounds, are given by:

- 186 1. Comfort performance index in the time-domain:

$$J_{comfort}^t = \int_0^\tau \ddot{z}_s^2(t) dt, \quad (12)$$

187 where τ represents a given time period.

- 188 2. Comfort performance index in the frequency-domain:

$$J_{comfort}^f = \frac{\mathcal{C}(f\{\ddot{z}_s^{controlled}\}, 0, 20)}{\mathcal{C}(f\{\ddot{z}_s^{nominal}\}, 0, 20)}, \quad (13)$$

189 where $\ddot{z}_s^{nominal}$ and $\ddot{z}_s^{controlled}$ refer to the car COG acceleration in a nominal (passive, uncontrolled)
 190 situation and when under a control scheme; moreover, $f\{\cdot\}$ represents the frequency response of the
 191 signal of interest, and $\mathcal{C} : \mathbb{R} \times \mathbb{R} \times \mathbb{R} \rightarrow \mathbb{R}$, denoted $\mathcal{C}(x, \underline{h}, \bar{h}) = \int_{\underline{h}}^{\bar{h}} |x(\mu)|^2 d\mu$, where \bar{h} and \underline{h} represent
 192 the frequency interval limits of interest.

193 2.2. Vehicle Testbed

194 For realistic validation purposes, when running numerical simulations, a full nonlinear vehicle model
 195 from [17] is used, which also embeds noises and couplings. This model has been validated and retrieved
 196 from a real mechatronic testbed.

197 This experimental platform from which the validation model has been constructed is the *INOVE Soben-*
 198 *Car*, a (1/5) reduced-size vehicle, show in Figure 3¹. The SA dampers in this testbed are Electro-Rheological
 199 (ER), which means that the PWM signal $u(t)$ controls an electric field which varies the viscosity of an ER
 200 fluid inside the damper chamber, increasing or decreasing the delivered force.

201 Table 1 presents the parameters from the quarter-car model in Eq (8) with respect to this testbed.

202 The real nonlinear behaviour of the ER SA dampers is shown in Figure 4 through Force vs. Deflection
 203 Speed diagrams, showing real data at the left side and fitted data at the right side, considering the use of
 204 Eq. (7) to compute the damper force. Clearly, the dissipativity constraints are respected if $u(t)$ is bounded
 205 to \mathcal{U} and Eq. (7) is used to compute the damper force.

206 *Remark 6.* The *INOVE Soben-Car* interprets control laws using a fixed sampling frequency of $f_s = 200$ Hz.
 207 This condition is quite restrictive in terms of implementation purposes, since the controller must always
 208 compute the control signal within 5 ms. Note that this sampling rate is realistic and adequate for actual
 209 top-cars [3].

¹Refer to full details in www.gipsa-lab.fr/projet/inove.



Figure 3: INOVE Soben-Car Mechatronic Testbed

Table 1: Vehicle Model Parameters

Parameter	Description	Value	Unit
m_s	Sprung mass	2.27	kg
m_{us}	Unsprung mass	0.32	kg
k_s	Spring stiffness	1396	N/m
k_t	Tire stiffness	12270	N/m
k_0	Passive damper stiffness	170.4	N/m
k_1	Hysteresis displacement coefficient	218.16	N/m
c_0	Viscous damping coefficient	68.83	N.s/m
c_1	Hysteresis velocity coefficient	21	N.s/m
f_c	Dynamic yield force of the ER fluid	28.07	N

210 2.3. Discrete-time qLPV Model

211 Since the SA suspension experimental testbed is evaluated with a fixed sampling frequency of $f_s = 200$ Hz,
 212 the controller must be synthesized with respect to a discrete-time model that embeds the $T_s = 5$ ms sampling
 213 period. Therefore, considering an Euler discretization method, the model is given by:

$$\begin{aligned}
 x(k+1) &= Ax(k) + B_1(\rho(k))u(k) + B_2w(k), \\
 y(k) &= Cx(k) + D_1(\rho(k))u(k) + D_2w(k), \\
 \rho(k) &= f_c \tanh(A_\rho x(k)),
 \end{aligned} \tag{14}$$

214 where² $w(k) = z_r(k)$, $A_\rho = [k_1 \ c_1 \ -k_1 \ -c_1]$, $A = \mathbb{I}_{n_x} + T_s A_c$, $B_1(\rho(k)) = T_s B_{c_1}(\rho(k))$ $B_2 =$
 215 $T_s B_{c_2}$, $C = C_c$, $D_1 = D_{c_1}$ and $D_2 = D_{c_2}$.

216 3. MPC Design for Systems with qLPV Models

217 The objective of this paper is to propose a control algorithm to enhance the comfort performances of
 218 the onboard passengers. This algorithm must be realizable and run within the 5 ms sampling period of the

²In this paper, \mathbb{I}_j denotes the identity matrix of dimension j .

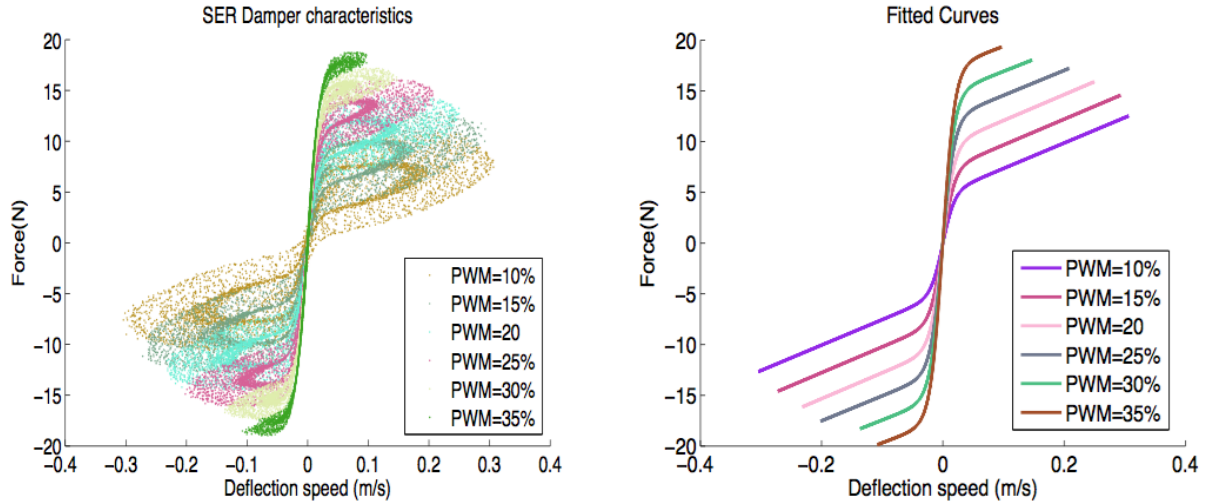


Figure 4: Force-Speed Characteristics - ER Semi-Active Dampers

219 considered SA suspension system. Moreover, the control policy must ensure input and state constraints are
 220 respected.

221 As discussed in the Introduction, MPC is a very elegant option for constrained processes and it is the
 222 method used in this paper. In this Section, a brief review on the available LPV MPC works is presented,
 223 highlighting why there is an intrinsic computational necessity increase with the size of the prediction horizon.
 224 The standard LPV MPC method is presented and the available approaches that lead to sub-optimality but
 225 overcome the numerical burden are presented.

226 3.1. Literature Overview

227 LPV MPC works are investigated since the beginning of the 00's; the majority of the methods consider
 228 that the scheduling parameter is an uncertain variable along the prediction horizon, solving the MPC problem
 229 robustly with respect to it. Some key papers are recalled:

- 230 • Explicit methods with stability and optimality guarantees were investigated in [29]. The downside
 231 is that, since the future values of the scheduling parameters are unknown, the algorithm ensures the
 232 constraints are satisfied for all possible system trajectories, which leads to conservative performances
 233 and (numerical-wise) high-demanding QPs.
- 234 • Dynamic output feedback algorithms have also been developed [30, 31]. Some of these papers use an
 235 LPV Input/Output representation. Anyhow, they are all robust towards ρ , solving worst-case (usually
 236 referred to as “min./max.”) optimization procedures and resulting in conservative results.
- 237 • Other papers [20, 32] present a major advance by considering bounded rates of the scheduling pa-
 238 rameters. This simple constraint simplifies the optimization procedure, treating the evolution of the
 239 scheduling parameters offline, via Linear Matrix Inequalities (LMIs) and ellipsoidal constraints. Their
 240 main downside is that the offline procedures are not necessarily simple to perform.
- 241 • Papers [33, 34] also consider bounded rates of the scheduling parameters, but the problem is formulated
 242 robustly with the use of “tubes” to deal with the uncertainty introduced by the scheduling parameters
 243 along the horizon. Recursive feasibility and stabilizability are demonstrated with respect to the tube
 244 formulation.
- 245 • That are also another group of papers that must be mentioned, those that parametrize the control
 246 inputs in finite amount of possible discrete values, solving a search algorithm to find the smallest cost
 247 instead of the actual optimization procedure [35, 36]

248 With regard to the previous methods, robust procedures or constraints are embedded to the MPC
 249 problem. To run these algorithms within 5 ms is, today, impossible. Therefore, some sub-optimal MPC
 250 works are recalled:

- 251 1. Both [37] and [38] use a frozen scheduling parameter trajectory guess that iterates according to mea-
 252 surements, and transform the nonlinear optimization problem into a linear one. The issue that resides
 253 with such methods is that the results may be sub-optimal and that the system trajectory might not
 254 be inside the region of attraction of the MPC, resulting in infeasibility.
- 255 2. In previous works, the Authors have also developed a QP version of the LPV MPC algorithm using
 256 a frozen parameter trajectory guess in [15, 39] and a Least-Squares (LS) identified parameter model
 257 in [22]. In the latter, a fictional set-point variable is used to enlarge the domain of attraction of the
 258 closed-loop system.

259 In this paper, the method developed in [22] is further extended and oriented towards the case of SA
 260 suspensions. In this paper, a Lyapunov-decreasing terminal cost and a the use of control invariant sets are
 261 added to the method to ensure that recursive feasibility is maintained for any starting condition within the
 262 constraints set \mathcal{X} , which addresses the issue of possible infeasibility from the previous work.

263 3.2. Why Embed Sub-Optimality?

264 Now, it is demonstrated why sub-optimal LPV MPC are needed for real-time implementation purposes.
 265 The regular MPC procedure is recalled:

266 MPC policies are essentially derived by solving an optimization procedure that takes into account con-
 267 straints on the states, outputs and control actions. With some bland assumptions, it is possible to guarantee
 268 closed-loop asymptotic stability for the LTI case [40]. Predictive control is widely used to achieve reference
 269 tracking and disturbance rejection performances in process control [9], by solving:

270 **Problem 1.** *Standard MPC Procedure*

$$\min_U J_{N_p} = \min_U \sum_{i=1}^{N_p} \ell(x, u) + V(x(k + N_p|k)) \quad (15)$$

$$s.t. \quad x(k + i + 1) = f(x(k + i), u(k + i), w(k + i)), \quad (16)$$

$$u(k + i - 1|k) \in \mathcal{U}, \quad (17)$$

$$x(k + i|k) \in \mathcal{X}, \quad (18)$$

271 where $U = \text{col}\{u(k|k), \dots, u(k + N_p - 1|k)\}$ is the sequence of actions inside the prediction horizon N_p ³.
 272 The MPC optimization cost J_{N_p} is comprised of the sum of a stage cost $\ell(\cdot)$ along the horizon and may
 273 also include a terminal stage value $V(x(k + N_p|k))$. J_{N_p} is usually Lyapunov-decreasing to ensure recursive
 274 feasibility. It is implied: $x \in \mathbb{R}^{n_x}$ and $u \in \mathbb{R}^{n_u}$, with \mathcal{X} and \mathcal{U} as the set constraints that define their
 275 respective feasible values (operation). The number of states is n_x and the number of control inputs is n_u .

276 *Remark 7.* The load disturbances $w(k) \in \mathbb{R}^{n_w}$ are assumed to be (partially) known for the future N_p steps.
 277 This is reasonable for the case of the automotive suspensions, as it will be further in the sequel. The number
 278 of disturbance variables is n_w .

279 When the system model is LTI, function $f(\cdot)$ is inherently linear and the optimization problem becomes
 280 a regular constrained QP, which is easily tackled by standard solvers. For the studied case, since the system
 281 model is qLPV, the optimization becomes nonlinear.

³Notation $(k + i|k)$ stands for a predictions for instant $k + i$, from the viewpoint of instant k . Consider \bar{U} and \underline{U} , respectively, as the maximal and minimal values this vector may assume.

282 **Definition 3.1.** Nonlinear Programming Problem

283 Consider an arbitrary real-valued nonlinear function $f_c(x_c)$. A nonlinear programming problem finds the
 284 vector x_c that minimizes $f_c(x_c)$ subject to $g_i(x_c) \leq 0$, $h_j(x_c) = 0$ and $x_c \in \mathcal{X}_c$, where g_i and h_j are also
 285 nonlinear.

286 **Definition 3.2.** Quadratic Programming Problem

287 A Quadratic Programming Problem (or simply Quadratic Problem, QP) is a linearly constrained mathe-
 288 matical optimization problem of a quadratic function. A QP is a particular type of nonlinear programming
 289 problems. The quadratic function may be defined with respect to several variables, all of which may be
 290 subject to linear constraints. Considering a $c \in \mathbb{R}^{n_c}$ vector, a symmetric matrix $Q_c \in \mathbb{R}^{n_c \times n_c}$, a real matrix
 291 $A_{ineq} \in \mathbb{R}^{m_c \times n_c}$, a real matrix $A_{eq} \in \mathbb{R}^{m_c \times n_c}$, a vector $b_{ineq} \in \mathbb{R}^{m_c}$ and another vector $b_{eq} \in \mathbb{R}^{m_c}$, the
 292 goal of a QP is to determine the vector $x_c \in \mathbb{R}^{n_c}$ that minimizes a regular quadratic function of form
 293 $\frac{1}{2}(x_c^T Q_c x_c + c^T x_c)$ subject to constraints $A_{ineq} x_c \leq b_{ineq}$ and $A_{eq} x_c = b_{eq}$. The solution x_c to this kind
 294 of problem is found by many solvers seen in the literature, based on Interior Point algorithms, quadratic
 295 search, etc.

296 Consider a generic discrete-time qLPV model $x(k+1) = A(\rho(k))x(k) + B(\rho(k))u(k)$, being the scheduling
 297 parameters endogenous, as gives $\rho(k) = f_\rho(x(k), u(k))$. These qLPV scheduling parameters are also possibly
 298 expressed through a dynamic recursive equation, i.e. $\rho(k) = f_\rho^m(\rho(k-1), \rho(k-2), \dots)$. The vector of future
 299 scheduling policies, from instant k , is given by:

$$\Gamma_k = \text{col}\{\rho(k+1), \rho(k+2), \dots, \rho(k+N_p-1)\}. \quad (19)$$

300 Then, departing from an arbitrarily feasible initial condition $x(k) = x_k$, Problem 1 has to internally
 301 elaborate constraint (16), which exhibits nonlinearities from the second iteration onward:

$$\begin{aligned} x(k+2|k) &= A(\rho(k+1))A(\rho(k))x_k \\ &+ A(\rho(k+1))B(\rho(k))u(k|k) + B(\rho(k+1))u(k+1|k). \end{aligned} \quad (20)$$

302 and so forth, up to the N_p -th prediction. This results, therefore, in non-QP version of Problem 1.

303 3.3. Frozen Scheduling Guess

304 Nonetheless, notice that these model-based predictions as in Eq. (20) would also be linear if ρ was known
 305 for every iteration inside the N_p horizon. To say one has knowledge of the complete future scheduling vector
 306 Γ_k is obviously false, since only $\rho(k)$ is known. But, if a frozen guess was to be used, as done in [15],
 307 substituting Γ_k by $\hat{\Gamma}_k$, Problem 1 would be translated into a QP version, but with sub-optimal results due
 308 to model-process mismatches, since the linear model use for predictions would be a frozen version of the
 309 qLPV process. Through the sequel, it is considered that the following Assumptions holds:

Assumption 3.3. *Some algorithm provides a guess for the evolution of the scheduling parameters along the horizon. This guess is denoted*

$$\hat{\Gamma}_k = \text{col}\{\hat{\rho}(k), \hat{\rho}(k+1), \dots, \hat{\rho}(k+N_p-1)\}.$$

310 *Remark 8.* It has been demonstrated in [22] that a recursive LS algorithm can be used to “predict” the
 311 scheduling parameters of a SA suspension system reasonably well.

312 **Assumption 3.4.** *As done in [20, 33], it holds that the ρ has a bounded variation rate, this is:*

$$\rho \in \mathcal{P} := [\underline{\rho}, \bar{\rho}] \text{ and } \dot{\rho} \in \delta\mathcal{P} := [\underline{\delta\rho}, \bar{\delta\rho}]. \quad (21)$$

313 *Remark 9.* In fact, as of Eq. (7), this is true, since $f_c \tanh(A_\rho x(k))$ is always bounded due to the fact that
 314 z_{def} is bounded. The derivative / difference is also inherently bounded.

315 From the viewpoint of k , the minimal and maximal prediction evolution guesses would be:

$$\hat{\Gamma}_k^{min} = \text{col}\{\rho(k) + \underline{\delta\rho}, \dots, \rho(k) + (N_p - 1)\underline{\delta\rho}\}, \quad (22)$$

$$\hat{\Gamma}_k^{max} = \text{col}\{\rho(k) + \overline{\delta\rho}, \dots, \rho(k) + (N_p - 1)\overline{\delta\rho}\}. \quad (23)$$

316 These bounds are taken into account by the LS algorithm as saturation limits. It is directly implied that
 317 $\hat{\Gamma}_k^{min} \subset \hat{\Gamma}_k \subset \hat{\Gamma}_k^{max}$

318 Let the generic discrete-time qLPV model be extended for the next j steps ahead of k^4 :

$$\begin{aligned} x(k+j) &= \overbrace{\prod_{n=0}^{j-1} A(\rho(k+n))}^{A^j(\Gamma_k)} x_k \\ &+ \underbrace{\sum_{m=1-k}^{j-k} \left(\left(\prod_{n=k+1}^{m-1} A(\rho(n)) \right) B(\rho(j-m)) u(j-m) \right)}_{B^j(\Gamma_k)U}. \end{aligned} \quad (24)$$

319 Then, since the scheduling prediction is always limited to the bounds given by $\hat{\Gamma}_k^{min}$ and $\hat{\Gamma}_k^{max}$, the model-
 320 process mismatches that arise by using a frozen model are also bounded. Take μ_j as these mismatches, due
 321 to the differences between the real state $x(k+j)$, which is a function of Γ_k , and the predicted state $\hat{x}(k+j)$,
 322 which is a function of the scheduling guess $\hat{\Gamma}_k$, as gives⁵:

$$\begin{aligned} \mu_j &= \hat{x}(k+j) - x(k+j) \\ &= \left(A^j(\hat{\Gamma}_k - \Gamma_k) \right) x_k \\ &+ \left(B^j(\hat{\Gamma}_k - \Gamma_k) \right) U, \end{aligned} \quad (25)$$

323 which leads to:

$$\begin{aligned} \underline{\mu}_j &\leq \mu_j \leq \overline{\mu}_j, \\ \underline{\mu}_j &= A^j(\hat{\Gamma}_k - \hat{\Gamma}_k^{min})x_k + B^j(\hat{\Gamma}_k - \hat{\Gamma}_k^{min})\underline{U}, \\ \overline{\mu}_j &= A^j(\hat{\Gamma}_k - \hat{\Gamma}_k^{max})x_k + B^j(\hat{\Gamma}_k - \hat{\Gamma}_k^{max})\overline{U}, \end{aligned} \quad (26)$$

324 where \overline{U} and \underline{U} represent, respectively, a sequence maximal and minimal control inputs.

325 Notice how these mismatches are bounded by the saturation conditions implied by the input constraints
 326 and a sequence of minimal or maximal scheduling parameter variations. Also, remark that μ_j increases
 327 along with the prediction horizon N_p , departing from $\mu_0 = 0$. This issue is rather interesting, since the
 328 MPC procedure will re-calculate the control sequences and predictions at each sampling instant, meaning
 329 that if the algorithm is recursively feasible, the effects of the model-process mismatches upon the controlled
 330 outputs will be relieved over time.

331 4. Set-Constrained Recursively Feasible qLPV MPC Procedure

332 Based on the discussion of the sub-optimal qLPV MPC design based on (bounded) frozen scheduling
 333 parameter evolution guesses $\hat{\Gamma}_k$ provided in the previous Section and the considered SA suspension appli-
 334 cation detailed in Sec. 2, this Section develops the proposed qLPV MPC algorithm for passenger comfort
 335 enhancement.

⁴ \prod stands for the left-side matrix product.

⁵Matrices $A^j(\cdot)$ and $B^j(\cdot)$ are affine in Γ_k . Therefore, $A^j(\hat{\Gamma}_k) - A^j(\Gamma_k) = A^j(\hat{\Gamma}_k - \Gamma_k)$.

336 A recursive saturated LS will provide, at each sampling instant k , an approximate guess for the evolution
 337 the scheduling parameters along the horizon. This frozen prediction $\hat{\Gamma}_k$ is passed to the MPC, that can be
 338 computed using a single QP.

339 Then, the design of such predictive controller must integrate some tools to guarantee reference-tracking
 340 despite the model uncertainties μ_j (that grow along the horizon). Essentially, what is done in this paper is
 341 to guarantee an enlarged domain of attraction of the system under closed-loop control, so that any initial
 342 condition that lies inside this domain can be steered as envisioned. Due to the horizon-increasing model-
 343 process mismatches μ_j , it must also guaranteed that the system is not driven out of an stability region,
 344 which can never be allowed. The recursive feasibility property must be verified to ensure that, although
 345 leading in sub-optimal results, the algorithm will stabilize and converge.

346 The tools used to address this matter are adapted to the qLPV case, respectively, from two prominent
 347 works [41, 40]: 1) the use of pseudo-reference tracking allows an enlargement of the domain of attraction of
 348 MPC policies, finding more options of stable closed-loop equilibrium points and 2) the usage of a terminal set
 349 that contracts along the horizon and a Lyapunov decreasing terminal stage cost, which together guarantee
 350 that, even with bounded uncertainties, the controlled system is able to meet performance goals whilst
 351 stability and feasibility are maintained.

352 *Remark 10.* These tools have previously been applied to the case of nonlinear systems; in [42], robust
 353 assessments are presented in terms of formal guarantees of recursivity and feasibility.

354 4.1. Pseudo-Reference Tracking

355 The “MPC for Tracking” method from [41] is considered in the sequel: this control design is used to
 356 ensure that the controller can asymptotically steer the process a steady-state reference x_s in an admissible
 357 manner from any feasible initial state x_0 . The approach consists basically in adapting the standard MPC
 358 cost function (i.e. weighting the quadratic difference between output and reference). The use of the “MPC
 359 for Tracking” design for qLPV models has been previously done in [43], where the scheduling trajectory Γ_k
 360 is taken as frozen, based on the known value $\rho(k)$ (no guess is performed).

361 *Remark 11.* The “MPC for Tracking” design includes an artificial reference x_a and sets the system to track
 362 it, while, at the same time, makes it track the actual reference x_s , which altogether ensures an enlarged
 363 domain of attraction. The target operation point $p_t = (x_s, u_s)$ is an admissible steady-state, which is
 364 possible if Eq. (14) is LPV-stabilizable (refer to the definition in [44]). Anyhow, this tool still does not
 365 guarantee the convergence of the qLPV system to the target point p_t because the model uncertainty μ_j
 366 is obviously non-null and horizon-increasing, as previously discussed. Therefore, a contractive terminal set
 367 constraint must also be used.

Assumption 4.1. Consider: (1) $Q \in \mathbb{R}^{n_x \times n_x}$ and $R \in \mathbb{R}^{n_u \times n_u}$ as positive definite matrices; and (2)
 $\kappa \in \mathbb{R}^{n_u \times n_x}$ as an arbitrary stabilizing state-feedback control gain. For these matrices, it is implied that,
 for the generic discrete-time qLPV model,

$$(A(\rho(k)) + B(\rho(k))\kappa)$$

is Schur. Then, there exists another positive definite matrix $P \in \mathbb{R}^{n_x \times n_x}$ such that

$$(A(\rho_k) + B(\rho_k)\kappa)^T P (A(\rho_k) + B(\rho_k)\kappa) - P = -(Q + \kappa^T R \kappa)$$

368 holds for all $\rho_k \in \Gamma_k$.

369 Then, as long as the previous Assumption holds, the MPC Problem is formulated with the following
 370 adjusted optimization cost:

$$J_{N_p} = V(\cdot) \tag{27}$$

$$+ \underbrace{\sum_{i=1}^{N_p} (\|x(k+i|k) - x_a\|_Q^2 + \|u(k+i-1|k) - u_s\|_R^2)}_{\text{Main Cost } \ell(\cdot)},$$

371 where the terminal stage cost is given by:

$$V(\cdot) = V_o^{x_a} + \overbrace{\|x(k + N_p|k) - x_a\|_P^2}^{V_o^x}, \quad (28)$$

372 with $x_a \in \mathcal{X}$ and $u_s \in \mathcal{U}$ being artificial variables for the set-point and for the control signal. The quadratic
 373 offset function $V_o^{x_a}$ penalizes the deviation between the artificial reference x_a and the target operation point
 374 x_s (actual set-point). The inclusion of a suitable penalization of the terminal state (terminal cost term V_o^x)
 375 can lead to asymptotic stability with good performances, as demonstrated in [42]. As pointed out by the
 376 latter, the offset cost $V_o^{x_s}$ must be convex and respect:

$$\beta_1 \|x_a - x_s\|_1 \leq V_o^{x_a}(x_a, x_s) \leq \beta_2 \|x_a - x_s\|_1, \quad (29)$$

377 where β_1, β_2 are positive real constants. The artificial tracking point is given by $p_s = (x_a, u_s)$.

378 **Proposition 4.2.** *If the stage cost weights Q and R are adequately chosen, is it possible to use an MPC*
 379 *algorithm, formulated with a quadratic stage cost of the form in Eq. (27), to optimize and enhance the*
 380 *comfort of onboard passengers, with respect to nominal (uncontrolled) situations.*

381 *Proof.* Indeed, MPC as a SA suspension control system can act to ensure a better comfort of the onboard
 382 passengers. The MPC will, at each sampling instant, act to minimize the primary control objective ℓ along
 383 the control horizon.

To do so, the time-domain index given in Eq. (12) is embedded to ℓ through Q and R . This index is re-written with respect to the discrete-time qLPV model in Eq. (14):

$$J_{comfort}^{N_p} = \sum_{j=0}^{N_p} \ddot{z}_s^2(k + j|k) T_s.$$

384 This finite sum approximates the integral in Eq. (12).

385 Then, assuming that (x_a, u_s) will converge to $(x_s, u_s) = (0, 0)$ (real set-point and respective control
 386 signal), it follows that⁶:

$$\begin{aligned} \sum_{j=0}^{N_p} \ddot{z}_s^2(k + j|k) T_s &= \sum_{j=0}^{N_p} \ell(\cdot) \\ &= \sum_{j=0}^{N_p} \|x(k + j|k)\|_Q^2 + \|u(k + j - 1|k)\|_R^2. \end{aligned} \quad (30)$$

387 From Eq. (14), it follows that:

$$\begin{aligned} \ddot{z}_s^2(k + j|k) T_s &= (C\{1, \cdot\}x(k + j - 1|k) \\ &+ D_1\{1, \cdot\}(\rho(k + j - 1|k)u(k + j - 1|k))^2 T_s. \end{aligned} \quad (31)$$

388 Thus, if Q and R are chosen, respectively, as:

$$Q = (C\{1, \cdot\})^T T_s (C\{1, \cdot\}), \quad (32)$$

$$R = (D\{1, \cdot\}(\rho_k))^T T_s (D\{1, \cdot\}(\rho_k)), \quad (33)$$

389 where $\rho(k + j - 1|k)$ is replaced by $\rho_k = \rho(k)$, for simplicity, the MPC policy with main cost $\ell(\cdot)$ will act
 390 to minimize $\ddot{z}_s^2(t)$ and enhance comfort performances. \square

⁶ $M\{l, \cdot\}$ denotes the vector formed by the l^{th} line of matrix M ; moreover, w is neglected from the sequence, since the control law has no measures over it (it cannot be minimized, since it is an external variable).

391 *Remark 12.* The objective of the inclusion of the artificial target point p_s works as follows. Consider that
 392 the system evolves as predicted (with $\mu_j = 0$) and that the actual target point $p_t = (x_s, u_s) = (0, 0)$ is an
 393 admissible point contained inside the tracking set $\mathcal{T} := \mathcal{X} \times \mathcal{U}$. Then, p_t is an asymptotically stable point in
 394 closed-loop, since the MPC will ensure convergence to it. Otherwise, the achieved closed-loop equilibrium is
 395 given by $p_s^* = (x_a^*, u_s^*) = \arg \min_{x_a} V_o^{x_a}(x_a, x_s)$. Moreover, the inclusion of the artificial reference ensures
 396 recursively feasibility properties of the algorithm and that the achieved closed-loop equilibrium x_a^* is the
 397 closest possible to x_s when it is feasible.

398 4.2. Contractive Sets

399 Consider the following definitions presented in [45]:

400 **Definition 4.3.** 1-Step Robust Set:

401 The 1-Step set of Υ , $\mathcal{Q}_1\{\Upsilon\}$, stands for the set of states which can be steered in one sampling instant into
 402 the target set Υ by an admissible control action, despite $\mu_j \neq 0$.

403 **Definition 4.4.** Robust Controlled Positively Invariant Set:

404 A set $\Upsilon \subset \mathbb{R}^{n_x}$ is said to be *control invariant* for the qLPV system in Eq. (14) if, for all possible $x_k \in \Upsilon$,
 405 there exists an admissible input $u = \kappa(x) \in \mathcal{U}$ so that $x(k+1)$ lies inside Υ despite $\mu_j \neq 0$. This is valid iff
 406 $\Upsilon \subseteq \mathcal{Q}_1\{\Upsilon\}$.

407 **Definition 4.5.** N_r -Step Control Invariant Sequence:

408 A sequence of N_r steps $\mathcal{S}_{N_r} := \{\Upsilon_j\}$ is the set sequence through which x can be steered through, leaping
 409 from one set Υ_j to the following Υ_{j-1} , with feasible control actions, until finally reaching the target invariant
 410 set Υ .

411 MPC design coupled to the use of control set sequences is used to make sure the algorithm guarantees
 412 asymptotic convergence despite model-process uncertainties μ_j , which is the case of this work⁷. To compute
 413 a reachable set sequences for qLPV models, the bounds on the variation rate of the scheduling parameters
 414 $\dot{\rho}$ must be taken into account: as gives Eq. (26), from the viewpoint of instant k , $x(k+1)$, for whichever
 415 $\rho(k+1) \in \mathcal{P}$, is, at most, equal to $x^*(k+1) = A(\rho^*)x_k + B_1(\rho^*)u(k)$ where $\rho^* = \rho(k) + \overline{d\rho}$ or $\rho^* = \rho(k) - \underline{d\rho}$.
 416 Therefore, Υ must be computed from x_k , abiding to:

$$417 \quad \Upsilon^{\text{Max}} \subseteq \Upsilon \subseteq \Upsilon^{\text{Min}} \quad \text{and} \quad p_t \in \Upsilon, \quad (34)$$

417 where Υ^{Max} and Υ^{Min} are the sets achieved with admissible control laws and, respectively, a sequence of
 418 N_r maximal and minimal scheduling parameter variations $\hat{\Gamma}_k^{\text{max}}$ and $\hat{\Gamma}_k^{\text{min}}$.

419 Then, for each iteration k , a sequence of reachable sets is computed as the intersection of the min./max.
 420 wider sets, found with $\hat{\Gamma}_k^{\text{max}}$ and $\hat{\Gamma}_k^{\text{min}}$, respectively. This is, for $j = \max\{N_r - k, 0\}, \dots, 0$:

$$421 \quad \mathcal{S}_{N_r} := \{ \text{col}\{\Upsilon_j\} \mid \Upsilon_j = (\Omega_j^{\text{max}} \cap \Omega_j^{\text{min}}) \}. \quad (35)$$

$$422 \quad \Omega_j^{\text{max}} = \left(A^{j+1}(\hat{\Gamma}_k^{\text{max}})x_k + B^{j+1}(\hat{\Gamma}_k^{\text{max}})U \right), \quad (36)$$

$$423 \quad \Omega_j^{\text{min}} = \left(A^{j+1}(\hat{\Gamma}_k^{\text{min}})x_k + B^{j+1}(\hat{\Gamma}_k^{\text{min}})U \right). \quad (37)$$

421 With these definitions in mind, to guarantee that within N_r steps from the initial instant k_0 the con-
 422 trolled qLPV system (14) reaches a terminal control invariant set Υ_0 in Eq. (34) which contains the target
 423 equilibrium p_t , the following contractive terminal set constraint is included to the design:

$$424 \quad x(k_0 + N_r) \in \Upsilon_j, \quad j = \max\{N_r - k, 0\}, \quad (38)$$

424 assuming \mathcal{S}_{N_r} is available from Eq. (35). Note that this terminal set Υ_j is equal to the larger Υ_{N_r} at the
 425 initial instant k_0 being shrunked subsequently until, at $k_0 + N_r$, it becomes the smallest set Υ_0 .

⁷For this development, $w(k+j)$ is suppressed, since it is a known variable throughout the N_p horizon.

426 *Remark 13.* This constraint makes the MPC method intrinsically time-varying, since, at least for the first
 427 N_r samples, the sets are contracting. In this paper, it is considered that $N_r \geq N_p$.

428 When the above terminal constraint is coupled to the MPC optimization procedure, there is indeed an
 429 enlargement of its domain of attraction, giving further holds on stability and feasibility, which are needed
 430 due to model-plant differences μ_j . The sequence of control invariant sets makes sure the terminal constraints
 431 contracts and the states converge to the desired target p_t (or as closely as possible, due to the pseudo-reference
 432 technique). Therefore, the main idea of the design method used in this paper is to use a constrained, finite
 433 horizon MPC to regulate the SA suspension system described by the discrete-time qLPV model in Eq. (14),
 434 from any admissible initial condition $x_0 \in \mathcal{X}$ to the target goal p_t using a fixed $\hat{\Gamma}_k$ by minimizing the
 435 adjusted objective function in Eq. (27) with $x(0, \rho(k)) \equiv x_0$ subject to the original constraints in Problem
 436 1 coupled to the contractive constraint in Eq. (38).

437 4.3. Quadratic Stabilizability and Recursive Feasibility

438 Since the terminal stage cost, terminal ingredient and primary optimization have been defined, it follows
 439 to verify if the proposed controller ensures quadratic stabilizability and recursive feasibility, which are
 440 envisioned properties of the algorithm.

441 **Definition 4.6.** Recursive Feasibility of MPC Algorithms[40]

442 Consider that the terminal set constraint on x exists such that $\Upsilon_0 \subset \mathcal{X}$, with \mathcal{X} closed, convex and compact
 443 and that the origin lies within the interior of Ω , for Ω being the largest admissible set⁸ such that $\Omega \subseteq \mathcal{X}$.
 444 Then, essentially, the following axioms verify if the MPC terminal cost function is Lyapunov-decreasing
 445 along the control horizon:

- 446 • A1) $\ell(\cdot) \geq \beta_1(\|x\|), \forall x \in \Omega, \forall u \in \mathcal{U}, \forall \rho \in \mathcal{P}$, for $\beta_1(\cdot)$ of class \mathcal{K}^9 .
- 447 • A2) $V(\cdot) \leq \beta_2(\|x\|), \forall x \in \Upsilon_0, \forall \rho \in \mathcal{P}$, for $\beta_2(\cdot)$ of class \mathcal{K}^{10} .
- 448 • A3) $V(x(k+1)) - V(x(k) + \ell(x(k), u(k))) \leq 0, \forall x \in \Upsilon_0, \forall u \in \mathcal{U}, \forall \rho \in \mathcal{P}, \forall k^{11}$.

449 If these three axioms hold. the MPC will be recursively feasible for any starting condition $x_0 \in \mathcal{X}$.

450 The terminal set Υ_0 is given by $\{x \in \mathbb{R}^{n_x} \mid V(x) \leq \alpha_s\}$ such that $\Upsilon_0 \subset \Omega$. Moreover, α_s is some scalar
 451 such that for all $x \in \Omega$, $f_m(x(k), u(k)) \in \Upsilon_0$.

452 **Definition 4.7.** Quadratic Stabilizability inside the Feasibility Region

453 The considered qLPV system given in Eq. (14) is said to be stabilizable if there exists a positive definite
 454 map $V : x(k) \rightarrow x(k)^T P x(k)$, where $P = P^T \succ 0$ and $P \in \mathbb{R}^{n_x \times n_x}$ and a state-feedback control policy
 455 of fashion $u(k) = \kappa x(k)$, with $\kappa \in \mathbb{R}^{n_u \times n_x}$, such that the following inequality:

$$V(A(\rho(k))x(k) + B(\rho(k))\kappa x(k)) - V(x(k)) \leq -x(k)^T (Q + \kappa^T R \kappa) x(k) \quad (39)$$

456 holds for all $x \in \mathcal{X}$ and $\rho \in \mathcal{P}$, with $Q = Q^T \succ 0$ and $R = R^T \succ 0$. Then, the origin is globally
 457 exponentially stable within the feasibility region \mathcal{X} is globally exponentially stable for $x(k+1) \forall \rho \in \mathcal{P}$ and
 458 any initial condition $x_0 \in \mathcal{X}$.

459 *Remark 14.* The above notion of quadratic stabilizability “inside the feasibility region” is slightly smoother
 460 than the notion of pure quadratic stabilizability, which would require the verification of the inequality for
 461 all $x \in \mathbb{R}^{n_x}$. The notion of the feasibility regionalization implies that only \mathcal{X} must be considered, which
 462 may be *a priori* a smaller proper \mathcal{C} set than \mathbb{R}^{n_x} (inequality must hold for all $x \in \mathcal{X}$ instead of \mathbb{R}^{n_x}).

⁸In fact, this set must also be positively control invariant, such that Ω is the one-step-step from Υ_0 .

⁹This axiom implies that ℓ is function-wise lower bounded.

¹⁰This axiom implies that V is function-wise upper bounded.

¹¹This axiom implies that V decreasing along the horizon.

463 **Definition 4.8.** \mathcal{K} refers to the class of positive and strictly increasing scalar functions that pass through
 464 the origin. A given function $f : \mathbb{R} \rightarrow \mathbb{R}$ is of class \mathcal{K} if $f(0) = 0$ and $\lim_{\xi \rightarrow +\infty} f(\xi) \rightarrow +\infty$.

465 **Assumption 4.9.** (i) There exists a \mathcal{K} function $\beta_1(\|x\|)$ that lower bounds the horizon cost $\ell(x)$; and (ii)
 466 there exists another \mathcal{K} function $\beta_2(\|x\|)$ that upper bounds the terminal cost $V(x(k + N_p))$.

467 **Proposition 4.10.** *Quadratic Stabilizability inside the Feasibility Region*
 468 *The considered qLPV system, when regulated by the MPC policy conducted through $u(k) = \kappa x(k)$ is quadratic*
 469 *stabilizable.*

470 *Remark 15.* The MPC policy yields a quadratic stabilizability property if the third recursive feasibility
 471 axiom verifies, with $V = x(k)^T P x(k)$, as demonstrated in the sequel. Moreover, full conditions for the
 472 satisfaction of A3 are demonstrated in [46], where LMI-solvable remedy to ensure this axiom is satisfied is
 473 proposed, concerning the case of scheduling parameter assumed as if they were held constant over N_p .

474 **Proposition 4.11.** *Recursive Feasibility*
 475 *The proposed algorithm is recursively feasible inside the feasibility set for any starting condition $x(k_0) =$*
 476 *$x_0 \in \mathcal{X}$.*

477 *Proof.* Since only the measured (state-feedback from an observer) variable $x(k)$ and scheduling sequence $\hat{\Gamma}_k$
 478 are used to solve Problem 1, at the following discrete-time instants $k > k_0 = 0$, the online optimization is
 479 not related to any disturbance variables and, thus, the recursive feasibility property can be analysed albeit
 480 disturbances (feedforward compensation is neglected in this proof).

481 Assume that Problem 1 is feasible for an initial condition x_0 , based on a Γ_{k_0} scheduling sequence,
 482 resulting in $U_{k_0}^*$ as the optimal sequence of control action which solves Eq. (15) at instant k_0 ; this optimal
 483 control policy leads to a minimal state sequence with respect to the cost function $J_{N_p}(\cdot)$. It holds that
 484 $x^*(k_0 + i) \in \Upsilon_j$ and $u(k_0 + i - 1|k_0) \in \mathcal{U} \forall i \in \mathbb{N}_{[1, N_p]}$. Moreover, it is implied that $x^*(k_0 + N_p) \in \Upsilon_0$,
 485 which is a positive invariant set for the qLPV model.

486 The MPC control policy $u(k_0) = u^*(k_0|k_0)$ is applied to the process and steers the system from the
 487 initial state x_0 to a successor state $x(k_0 + 1) = \hat{x}^*(k_0 + 1|k_0) = x^*(k_0 + 1|k_0) = x^*$. Next, it is demonstrated
 488 that, at instant $k_1 = k_0 + 1$, for initial condition $x_1 = x(k_1)$ and scheduling sequence Γ_{k_1} , there exists a
 489 feasible solution to Problem 1. The feasibility of the solution at instant k_0 is used to construct a feasible
 490 solution at this following sample k_1 .

491 Take the bounds of the variation of the scheduling parameters into account, as follows:

$$x(k_1 + 1) = A(\rho(k_1))x_1 + B_1(\rho(k_1))u(k_1), \quad (40)$$

492 since $u(k_1) = \kappa x_1 = \kappa x^*$ and $\rho(k_1) = \rho(k_0) + \sum_{l=0}^{k_1-k_0} \partial\rho(l)$, one arrives at:

$$\begin{aligned} x(k_1 + 1) &= A(\rho(k_0) + \partial\rho(k_0))x^* + B_1(\rho(k_0) + \partial\rho(k_0))\kappa x^* \\ &= [A(\rho(k_0) + \partial\rho(k_0)) + B_1(\rho(k_0) + \partial\rho(k_0))\kappa] x^* \\ &= \underbrace{(A(\rho(k_0) + B_1(\rho(k_0))\kappa))}_{A_{cl}(\rho(k_0), x^*)} x^* \\ &\quad + \underbrace{(A(\partial\rho(k_0)) + B_1(\partial\rho(k_0))\kappa)}_{w(k_1)} x^*. \end{aligned}$$

493 Since $w(k_1)$ is ultimately bounded due to its construction (given that μ_j is bounded and residing on the
 494 fact that scheduling parameters variation rates are also bounded), $\partial\rho \leq \partial\rho(k) \leq \bar{\partial\rho}$, and the bounds on x
 495 (i.e. $x \in \mathcal{X}$), it holds that $x(k_1 + 1)$ is indeed an admissible point, contained inside the feasibility set for x
 496 (it does not diverge), this is: $A_{cl}(\rho(k_0), x^*)x^* + w(k_1) \in \mathcal{X}$.

497 Finally, apart from this induction development, the three recursive feasibility axioms will also be verified
 498 individually:

499 A1) Indeed $\ell(x)$ is \mathcal{K} -class lower bounded, i.e.¹²:

$$\begin{aligned}
\ell(x) &= (x(k+i)^T Q x(k+1) + u(k)^T R u(k)) \\
&= (A(\rho)x + B_1(\rho)u)^T Q (A(\rho)x + B_1(\rho)u) + x^T \kappa^T R \kappa x \\
&= x^T (A(\rho)^T Q A(\rho) + 2A^T(\rho) Q B_1(\rho) \kappa \\
&\quad + \kappa^T B^T(\rho) Q B_1(\rho) \kappa + \kappa^T R \kappa) x \\
&= x^T (A_\ell(\rho, x)) x \geq x^T \beta_1 x = \beta_1(\|x\|),
\end{aligned} \tag{41}$$

500 which means that it is always possible to choose a real constant scalar β_1 which is $\leq A_\ell(\rho, \underline{x}) \forall x \in \Omega = \Upsilon_1$.

501 A2) Indeed the terminal stage cost $V(\cdot)$ is \mathcal{K} -class upper bounded; departing from $x(0) = x$, it follows¹³:

$$\begin{aligned}
V(x(k+N_p)) &= x^T(k+N_p) P x(k+N_p) \\
&= \left(A^{N_p}(\Gamma_k) x + B_1^{N_p}(\Gamma_k) \kappa \vec{X}_{k, N_p} \right)^T P \\
&\quad \left(A^{N_p}(\Gamma_k) x + B_1^{N_p}(\Gamma_k) \kappa \vec{X}_{k, N_p} \right) \\
&= x^T \overbrace{\left(A^{N_p}(\Gamma_k) P A^{N_p}(\Gamma_k) \right)}^{A_V(\Gamma_k)} x \\
&\quad + 2x^T \overbrace{\left((A^{N_p}(\Gamma_k))^T P B_1^{N_p}(\Gamma_k) \kappa \right)}^{h(\Gamma_k, \vec{X}_{k, N_p})} \vec{X}_{k, N_p} \\
&\quad + \vec{X}_{k, N_p}^T \overbrace{\left(\kappa^T (B_1^{N_p}(\Gamma_k))^T P B_1^{N_p}(\Gamma_k) \kappa \right)}^{B_V(\Gamma_k, \vec{X}_{k, N_p})} \vec{X}_{k, N_p} \\
&\leq x^T \beta_2 x = \beta_2(\|x\|),
\end{aligned} \tag{42}$$

502 which means that it is always possible to find a real constant scalar

$$\begin{aligned}
\beta_2 &\geq (A_V(\Gamma_k) + 2h(\Gamma_k^{max}, \vec{X}_{k, N_p}, \vec{A}_{k, N_p}) \\
&\quad + \vec{A}_{k, N_p}^T B_V(\Gamma_k^{max}, \vec{X}_{k, N_p}, \vec{A}_{k, N_p}), \forall x \in \Upsilon_0.
\end{aligned}$$

503 A3) Finally, the last axiom is verified: consider $x(k+j+1) = x(k+1)$ and $x(k+j) = x$, for notation
504 simplicity, which is valid for all $j \in 0, \dots, N_p - 1$. The terminal ingredient should be decrescent along the
505 solution of x . Of course, the use of the contracting terminal constraints $x(k+N_p|k) \in \Upsilon_j$, implies that
506 the state trajectories are steered further towards the QP target set goal as k increases, this, by itself, should
507 guarantee that V is decrescent[47, 41]. The decay of $V(\cdot)$ is demonstrated:

$$\begin{aligned}
V(x(k+1)) - V(x) + \ell(x) &\leq 0 \\
x(k+1)^T P x(k+1) - x^T P x + x^T (A_\ell(\Gamma_k, x)) x &\leq 0 \\
x^T (A(\rho(k))^T P A(\rho(k)) + 2A(\rho(k)) P B(\rho(k)) \kappa \\
&\quad + \kappa^T B^T(\rho(k)) P B(\rho(k)) \kappa) x \\
&\quad - x^T P x + x^T (A_\ell(\Gamma_k, x)) x &\leq 0,
\end{aligned}$$

¹²Notation is simplified, the $(k+i)$ is dropped.

¹³Notation $\vec{X}_{k,j}$ denotes the collection of sequence of states from $x(k)$ to $x(k+j)$.

508 which is equivalent to:

$$\begin{aligned}
& (A^T(\rho(k))(P + Q)A(\rho(k)) - P) \\
& + (\kappa^T B^T(\rho(k))(P + Q)A(\rho(k)) \\
& + A^T(\rho(k))(P + Q)B(\rho(k))\kappa) \\
& + (\kappa^T B^T(\rho(k))(P + Q)B(\rho(k))\kappa) \\
& \leq \kappa^T R \kappa,
\end{aligned}$$

509 which is inherently verified due to the choice of P under Assumption 4.1, being Q also full-rank and positive
510 definite by definition. This concludes proof. \square

511 4.4. Implementation Remarks

512 This Section presented an MPC design procedure for the control of SA suspension systems, aiming to
513 enhance passenger comfort performances. This procedure converts the nonlinear optimization problem with
514 the original qLPV model into an LTI-scheduled model and QP complexity. To make sure the simplifications
515 of using a scheduling trajectory guess do not compromise the control performances, a pseudo-reference and
516 control invariant set sequences are used s.t. feasibility is guaranteed. This MPC design is sub-optimal
517 due to model-process mismatches, but it has a major advantage of using a single QP, which makes it
518 computationally practicable under the 5 ms sampling period of the vehicle.

519 For the implementation of the algorithm, it is assumed that the road profile (load disturbances) $w(k)$
520 are known for the future N_r steps. This information can be pursued with different schemes from the
521 literature, such as frequencial preview loops, adaptative estimation schemes or even extended observers that
522 estimate the road together with the states. Some options for these algorithms are available in [48, 5, 17, 49].
523 Notice that when computing the terminal set sequences, the road profile information is embedded. The
524 implementation of the proposed MPC algorithm is described in Algorithm 1.

525 5. Numerical Results

526 In the Section, numerical simulation results are presented to illustrate the performances of a SA sus-
527 pension system under the control of the proposed qLPV MPC algorithm. The following results have been
528 obtained with textitMatlab, *Yalmip* toolbox and *Gurobi* solver. The simulation is performed with a realis-
529 tic, validated, full vehicle nonlinear model of the experimental testbed of a vehicle equipped with four ER
530 dampers.

531 Once again, recall that the control input for the SA suspension system is the PWM signal $u(t)$, which
532 varies the damping coefficient of the ER dampers by changing the electric field applied over them, which
533 varies the amount of force that is delivered.

534 Recall that the primary control objective $\ell(\cdot)$ is taken in order to minimize chassis accelerations, to ensure
535 that a smoother ride is provided and the comfort of the passengers is enhanced. The indexes provided in
536 Section 2.1 will be used to evaluate the enhancement provided by the proposed control scheme.

537 In the following Figures, the proposed method is denoted “qLPVMPC”, while “COLQR” denotes a
538 clipped optimal LQR, computed with the LTI versions (frozen $\hat{\Gamma}_k$) of the qLPV process and the same
539 weights Q, R and P . The results obtained with a purely passive, uncontrolled SA damper are marked as
540 “PDamp” (for this, u is taken as null).

541 According to [17], the prediction horizon N_p is taken as 10 samples, while the contractive horizon N_r
542 is taken as 25, meaning that the positively invariant control sets shrink 2.5 times slower than the sliding
543 horizon. For evaluation of the control strategy itself, the computational processing time for the sequence of
544 sets is excluded from the nominal elapsed time of the algorithm, since they could have been performed all
545 offline, as done in [50].

546 The following results consider the SA suspension at the front-left corner of the vehicle. Similar results
547 were obtained for the other three corners. The chosen road profile $z_r(t) = w(t)$ stands for a car running in
548 a straight line on a dry road, when it encounters ($t' = 0.5$ s) a sequence of 5 mm bumps on all its wheels,

Algorithm 1 LPV MPC for Passenger Comfort Enhancement

1. Use some estimation algorithm to get the future values for the road profile disturbances w along the next N_r steps;
2. Use a saturated recursive LS procedure to estimate the scheduling parameters of the system along the horizon $\hat{\Gamma}_k$, these parameters represent a hyperbolic tangent function of the deflection velocity and suspension deflection variables;
3. Compute the LTI model that approximates the process along the horizon, based on the scheduling evolution guess $\hat{\Gamma}_k$ for $j = 1, \dots, N_p$.
4. Compute the final set that contains the desired reference Υ_0 according to Eq. (34). This step has also a QP complexity, see [41];
5. Loop with $i = 1 : 1 : N_r$, from $k = k_0$:
6. Compute the sequence Υ_j of $(N_r - i)$ sets, according to Eq. (35). These sequences of sets are computed using relaxations/contractions from the present state until the target final set Υ_0 .
7. Solve the following QP:

$$\begin{aligned} \min_U \quad & J_N(x, u) & (43) \\ \text{s.t.} \quad & \text{System Evolution: Eq. (14),} \\ & u(k+i-1|k) \in \mathcal{U}, \\ & x(k+i|k) \in \mathcal{X}, \\ & x(k+N_r|k) \in \Upsilon_j, \quad j = \max\{N_r - k, 0\}, \end{aligned}$$

8. From U , take the first entry $u(k|k) = \kappa x(k)$ and apply it to the process.
-

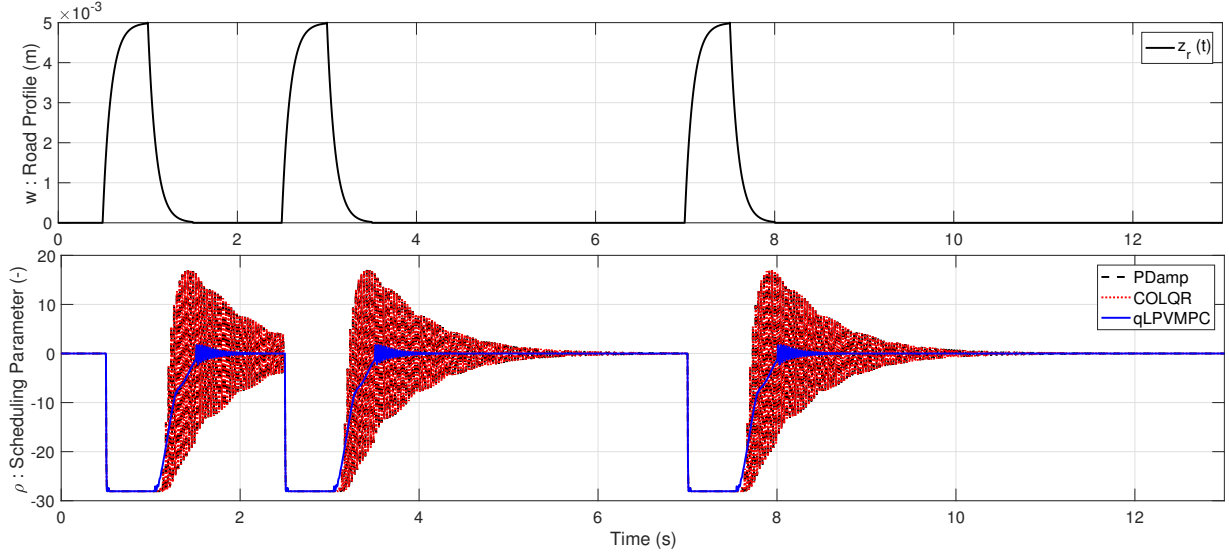


Figure 5: Road Profile and Scheduling Parameters

549 exciting the bounce motion, which must be counteracted by the suspension controller. This simulation
 550 scenario comprises 13 s. Figure 5 shows these bumps and the scheduling parameters along the simulation.

551 Most importantly, Figure 6 depicts both controlled outputs ($\ddot{z}_s, \ddot{z}_{us}$) and the delivered damping force
 552 (as well as the dissipativity constraints \mathcal{D}). Clearly, it is evident that the proposed predictive controller
 553 yields the smoother results, further minimizing the control objective $\ell(\cdot)$. Due to saturation effects, the
 554 LQR strategy achieved almost the results as those with a passive damper (in open-loop).

555 To better evaluate these results, the time index $J_{comfort}^t$ is computed through a normalized root-mean-
 556 square (RMS) function of the acceleration variables. Table 2 shows the RMS obtained for the passive case
 557 for both $\ddot{z}_s(t)$ and $\ddot{z}_{us}(t)$ and the enhancements achieved with the COLQR and qLPVMPC methods with
 558 respect to the passive condition. As evidenced, the proposed method yields a 14.25% passenger comfort
 559 enhancement in terms of the chassis acceleration variable. This is quite significant as it the algorithm is
 560 computed for a scaled vehicle model.

Table 2: Performance Enhancement

RMS	Method	Value	Enhancement
Reference	PDamp	0.4650	0%
Tracking	COLQR	0.4646	0.08%
$\ddot{z}_s(t) \rightarrow 0$	qLPVMPC	0.3984	14.32%
Reference	PDamp	3.008	0%
Tracking	COLQR	3.005	0.1%
$\ddot{z}_{us}(t) \rightarrow 0$	qLPVMPC	2.611	13.18%

561 Concerning the frequencial index $J_{comfort}^f$, Figure 7 shows the FFT results of $\ddot{z}_s(t)$ for both PDamp and
 562 qLPVMPC cases, under the 0–20 Hz frequency range. As discussed by [12], the important issue is to reduce
 563 the peaks caused when a road profile income appears. In numerical terms, the peak with the qLPVMPC
 564 method is 16.25% smaller than the one with the passive damper, which demonstrates furthermore the
 565 enhancement provided to the passengers.

566 It must be remarked that the proposed method with its sets computations can be performed using parallel

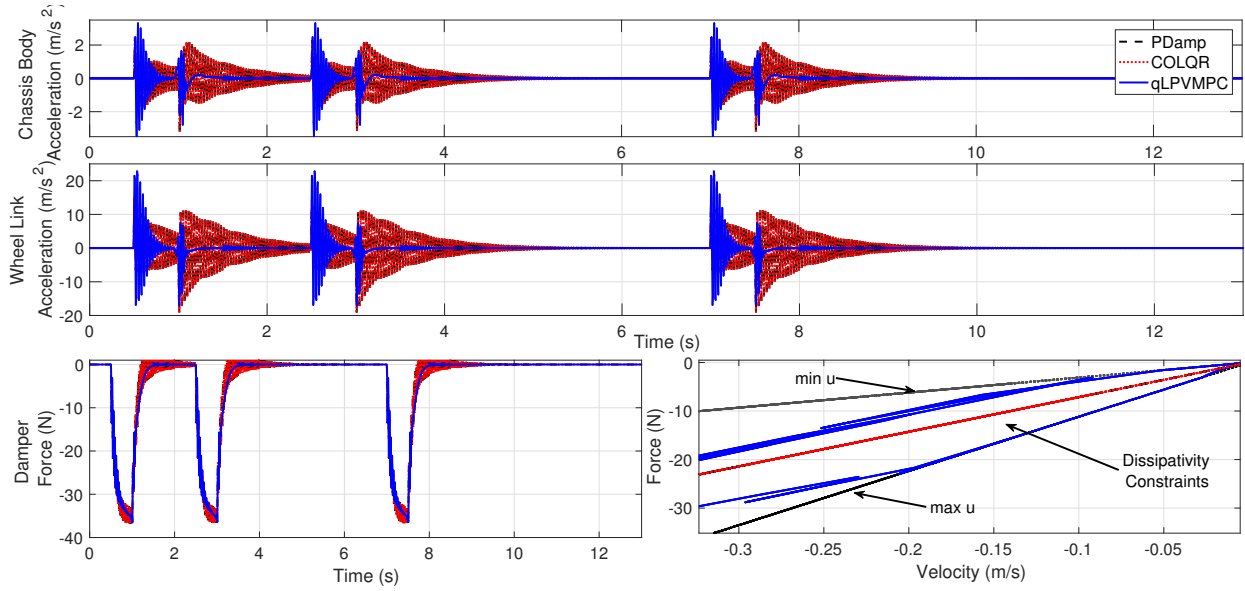


Figure 6: Controlled Outputs and Control Signal

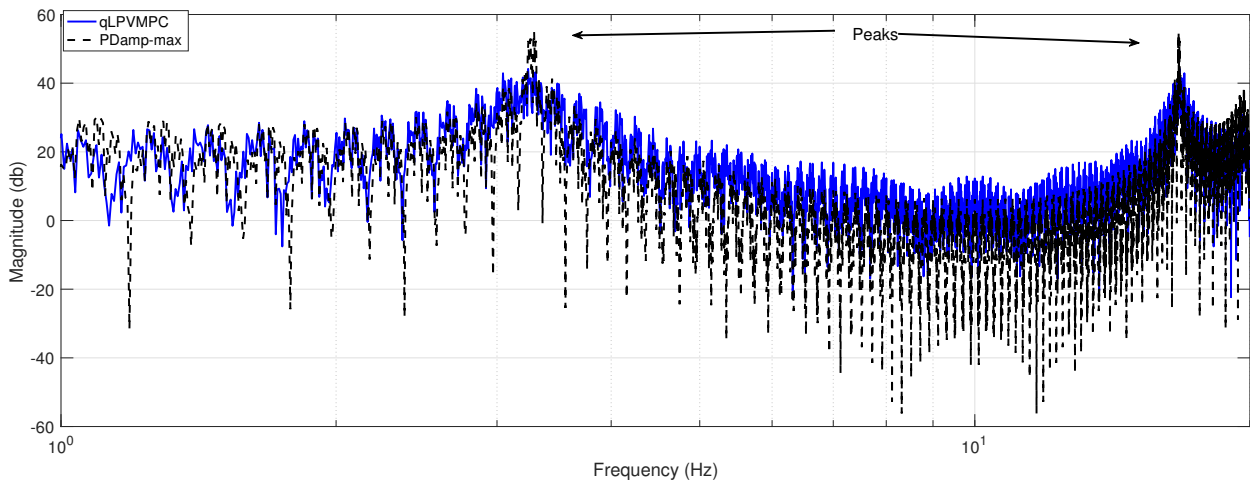


Figure 7: FFT: $J_{comfort}^f$

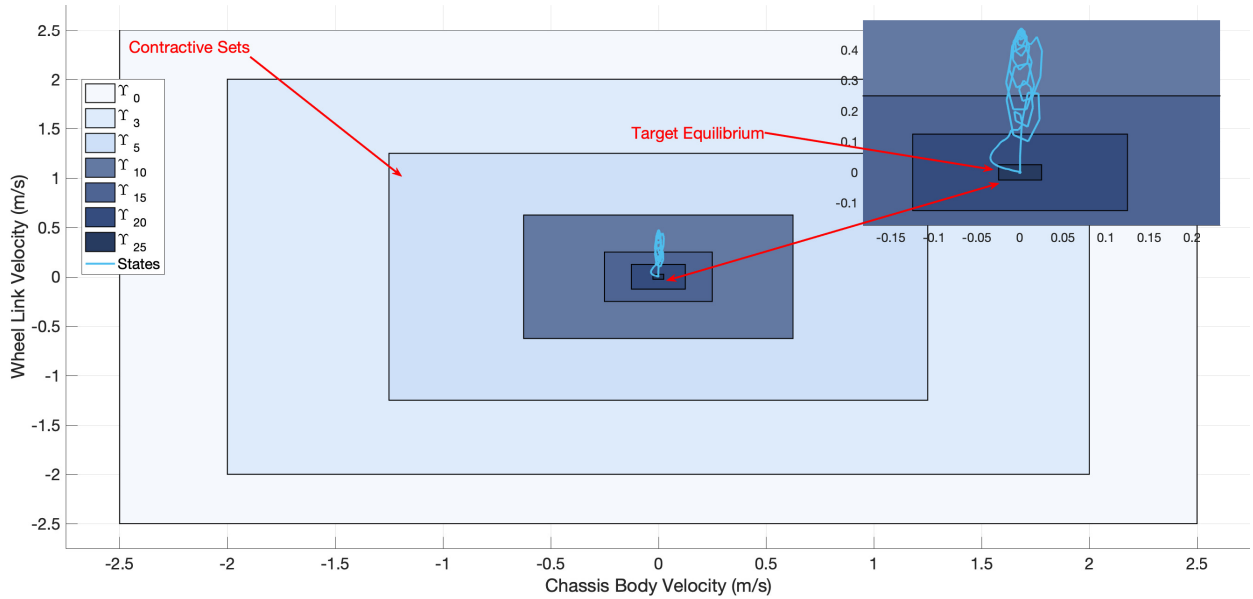


Figure 8: Controlled Outputs Tracking Plane

567 computing tools; in fact, this QP step that is used to compute the control law (Step 7 of the Algorithm
 568 in Section 4.4) allows to achieve a quite reasonable numerical effort (elapsed within $0.035\text{ s} < T_s$). If the
 569 original nonlinear programming problem was to be considered (without the frozen guess for the scheduling
 570 parameter), much greater effort would be necessary and the law would not be able to be implemented for
 571 real-time purposes.

572 Concerning the qLPV results, some additional results must be presented: Figure 8 shows a $\dot{z}_s(t) \times \dot{z}_{u.s}(t)$
 573 plane and the (2D-cut) contracting sets Υ_j . Clearly, the sets tool works to constrain the convergence of
 574 these velocities to a (target) final region, despite the disturbance and model-process mismatches. Finally,
 575 Figure 9 shows a 3D polyhedra cut version of Υ_{N_r} (which is, in fact, 4D) and the polyhedra obtained for
 576 the evolution of the last three states; this Figure demonstrates how the initial polyhedra contains the state
 577 evolutions, which finally converge to Υ_0 . This result also corroborates with the validity of the recursive
 578 feasibility axioms (specially A3).

579 6. Conclusions

580 This paper elaborated a novel MPC method for the enhancement of passenger comfort using SA sus-
 581 pension systems. The suspension is modelled within a qLPV framework, and the damping force is modelled
 582 through a nonlinear hyperbolic tangent function, as suggested by the literature. The method embed the
 583 nonlinearities within a scheduling parameter, which is estimated through the prediction horizon at each
 584 sampling instant. The frozen scheduling evolution guess is used to transform the nonlinear prediction prob-
 585 lem into a linear QP, which can be solved within some mili-seconds. Set-based tools (terminal ingredient
 586 and stage cost) are included to the MPC so that it maintains quadratic stability and recursive feasibility,
 587 despite model-process mismatches. These properties are analytically demonstrated. The optimization cost
 588 function of the MPC is shown to embed comfort constraints, with regard to performance indexes from
 589 the literature. The algorithm is successfully applied to the control of a Semi-Active suspension system via
 590 realistic simulation, achieving good results compared to existing control optimal control methods.

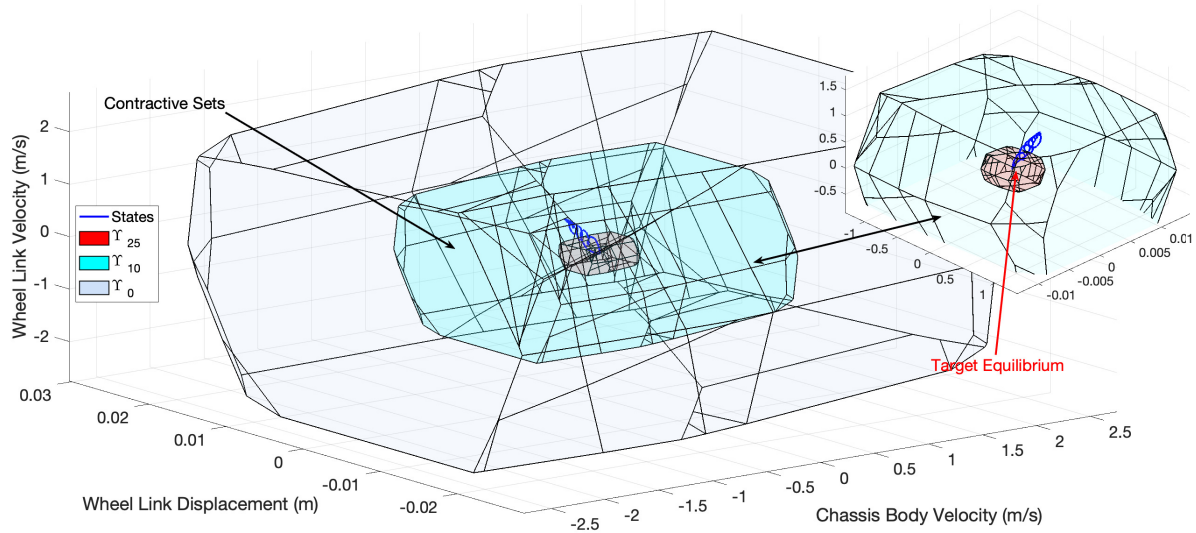


Figure 9: Polyhedra Υ_j and states

591 Acknowledgments

592 This work has been supported by CNPq project 304032/2019 – 0 and ITEA3 European project 15016
 593 EMPHYSIS (Embedded Systems With Physical Models in the Production Code Software).

594 References

- 595 [1] Fischer, D., Isermann, R.: ‘Mechatronic semi-active and active vehicle suspensions’, *Control engineering practice*, 2004,
 596 **12**, (11), pp. 1353–1367
- 597 [2] Savaresi, S.M., Poussot.Vassal, C., Spelta, C., Sename, O., Dugard, L.: ‘Semi-active suspension control design for vehicles’.
 598 Butterworth-Heinemann. Elsevier, 2010)
- 599 [3] Poussot.Vassal, C., Spelta, C., Sename, O., Savaresi, S.M., Dugard, L.: ‘Survey and performance evaluation on some
 600 automotive semi-active suspension control methods: A comparative study on a single-corner model’, *Annual Reviews in*
 601 *Control*, 2012, **36**, (1), pp. 148–160
- 602 [4] Tseng, H.E., Hrovat, D.: ‘State of the art survey: active and semi-active suspension control’, *Vehicle system dynamics*,
 603 2015, **53**, (7), pp. 1034–1062
- 604 [5] Unger, A., Schimmack, F., Lohmann, B., Schwarz, R.: ‘Application of LQ-based semi-active suspension control in a
 605 vehicle’, *Control Engineering Practice*, 2013, **21**, (12), pp. 1841–1850
- 606 [6] Nguyen, M.Q., da Silva, J.G., Sename, O., Dugard, L.: ‘A state feedback input constrained control design for a 4-semi-
 607 active damper suspension system: a quasi-LPV approach’, *IFAC-PapersOnLine*, 2015, **48**, (14), pp. 259–264
- 608 [7] Poussot.Vassal, C., Sename, O., Dugard, L., Gaspar, P., Szabo, Z., Bokor, J.: ‘A new semi-active suspension control
 609 strategy through LPV technique’, *Control Engineering Practice*, 2008, **16**, (12), pp. 1519–1534
- 610 [8] Pang, H., Zhang, X., Xu, Z.: ‘Adaptive backstepping-based tracking control design for nonlinear active suspension system
 611 with parameter uncertainties and safety constraints’, *ISA transactions*, 2019, **88**, pp. 23–36
- 612 [9] Camacho, E.F., Bordons, C.: ‘Model predictive control’. Springer Science & Business Media, 2013)
- 613 [10] Allgöwer, F., Zheng, A.: ‘Nonlinear model predictive control’. vol. 26. Birkhäuser, 2012)
- 614 [11] Nguyen, M.Q., Canale, M., Sename, O., Dugard, L.: ‘A model predictive control approach for semi-active suspension
 615 control problem of a full car’. In: IEEE 55th Conference on Decision and Control. IEEE, 2016. pp. 721–726
- 616 [12] Poussot.Vassal, C., Savaresi, S.M., Spelta, C., Sename, O., Dugard, L.: ‘A methodology for optimal semi-active suspension
 617 systems performance evaluation’. In: 49th IEEE Conference on Decision and Control. IEEE, 2010. pp. 2892–2897
- 618 [13] Giorgetti, N., Bemporad, A., Tseng, H.E., Hrovat, D.: ‘Hybrid model predictive control application towards optimal
 619 semi-active suspension’, *International Journal of Control*, 2006, **79**, (05), pp. 521–533
- 620 [14] Brezas, P., Smith, M.C., Hoult, W.: ‘A clipped-optimal control algorithm for semi-active vehicle suspensions: Theory and
 621 experimental evaluation’, *Automatica*, 2015, **53**, pp. 188–194
- 622 [15] Morato, M.M., Sename, O., Dugard, L.: ‘LPV-MPC fault tolerant control of automotive suspension dampers’, *IFAC-
 623 PapersOnLine*, 2018, **51**, (26), pp. 31–36

- 624 [16] Beal, C.E., Gerdes, J.C.: ‘Model predictive control for vehicle stabilization at the limits of handling’, *IEEE Transactions*
625 *on Control Systems Technology*, 2013, **21**, (4), pp. 1258–1269
- 626 [17] Morato, M.M., Nguyen, M.Q., Sename, O., Dugard, L.: ‘Design of a fast real-time LPV model predictive control system
627 for semi-active suspension control of a full vehicle’, *Journal of the Franklin Institute*, 2018,
- 628 [18] Sename, O., Gaspar, P., Bokor, J.: ‘Robust control and linear parameter varying approaches: application to vehicle
629 dynamics’. vol. 437. Springer, 2013)
- 630 [19] Mohammadpour, J., Scherer, C.W.: ‘Control of linear parameter varying systems with applications’. Springer Science &
631 Business Media, 2012)
- 632 [20] Jungers, M., Oliveira, R.C., Peres, P.L.: ‘MPC for LPV systems with bounded parameter variations’, *International*
633 *Journal of Control*, 2011, **84**, (1), pp. 24–36
- 634 [21] Abbas, H.S., Toth, R., Petreczky, M., Meskin, N., Mohammadpour, J.: ‘Embedding of nonlinear systems in a linear
635 parameter-varying representation’, *IFAC Proceedings Volumes*, 2014, **47**, (3), pp. 6907–6913
- 636 [22] Morato, M.M., Normey-Rico, J.E., Sename, O.: ‘Novel qLPV MPC design with least-squares scheduling prediction’. In:
637 Proceedings of the 3th IFAC Workshop on Linear Parameter Varying Systems, Eindhoven, The Netherlands, Nov. 4-6,
638 2019.
- 639 [23] Morato, M.M., Sename, O., Dugard, L., Nguyen, M.Q.: ‘Fault estimation for automotive electro-rheological dampers:
640 LPV-based observer approach’, *Control Engineering Practice*, 2019, **85**, pp. 11–22
- 641 [24] Guo, S., Yang, S., Pan, C.: ‘Dynamic modeling of magnetorheological damper behaviors’, *Journal of Intelligent material*
642 *systems and structures*, 2006, **17**, (1), pp. 3–14
- 643 [25] Ren, H., Chen, S., Zhao, Y., Liu, G., Yang, L.: ‘State observer-based sliding mode control for semi-active hydro-pneumatic
644 suspension’, *Vehicle System Dynamics*, 2016, **54**, (2), pp. 168–190
- 645 [26] Falcone, P., Tseng, H.E., Asgari, J., Borrelli, F., Hrovat, D.: ‘Integrated braking and steering model predictive control
646 approach in autonomous vehicles’, *IFAC Proceedings Volumes*, 2007, **40**, (10), pp. 273–278
- 647 [27] Beal, C.E., Gerdes, J.C.: ‘Model predictive control for vehicle stabilization at the limits of handling’, *IEEE Transactions*
648 *on Control Systems Technology*, 2012, **21**, (4), pp. 1258–1269
- 649 [28] Hrovat, D.: ‘Survey of advanced suspension developments and related optimal control applications’, *Automatica*, 1997,
650 **33**, (10), pp. 1781–1817
- 651 [29] Besselmann, T., Lofberg, J., Morari, M.: ‘Explicit MPC for LPV systems: Stability and optimality’, *IEEE Transactions*
652 *on Automatic Control*, 2012, **57**, (9), pp. 2322–2332
- 653 [30] Abbas, H.S., Hanema, J., Tóth, R., Mohammadpour, J., Meskin, N.: ‘A new approach to robust MPC design for LPV
654 systems in input-output form’, *IFAC-PapersOnLine*, 2018, **51**, (26), pp. 112–117
- 655 [31] Ding, B., Ping, X., Pan, H.: ‘On dynamic output feedback robust MPC for constrained quasi-lpv systems’, *International*
656 *Journal of Control*, 2013, **86**, (12), pp. 2215–2227
- 657 [32] Casavola, A., Famularo, D., Franzè, G., Garone, E.: ‘A fast ellipsoidal MPC scheme for discrete-time polytopic linear
658 parameter varying systems’, *Automatica*, 2012, **48**, (10), pp. 2620–2626
- 659 [33] Hanema, J., Tóth, R., Lazar, M.: ‘Stabilizing non-linear MPC using linear parameter-varying representations’. In: 56th
660 Annual Conference on Decision and Control. IEEE, 2017. pp. 3582–3587
- 661 [34] Hanema, J., Lazar, M., Tóth, R.: ‘Stabilizing tube-based model predictive control: Terminal set and cost construction for
662 LPV systems’, *Automatica*, 2017, **85**, pp. 137–144
- 663 [35] Rathai, K.M.M., Alamir, M., Sename, O., Tang, R.: ‘A parameterized NMPC scheme for embedded control of semi-active
664 suspension system’, *IFAC-PapersOnLine*, 2018, **51**, (20), pp. 301–306
- 665 [36] Alamir, M.: ‘A framework for real-time implementation of low-dimensional parameterized NMPC’, *Automatica*, 2012, **48**,
666 (1), pp. 198–204
- 667 [37] Cisneros, P.S., Sridharan, A., Werner, H.: ‘Constrained predictive control of a robotic manipulator using quasi-LPV
668 representations’, *IFAC-PapersOnLine*, 2018, **51**, (26), pp. 118–123
- 669 [38] Alcalá, E., Puig, V., Quevedo, J.: ‘LPV-MPC control for autonomous vehicles’, *IFAC-PapersOnLine*, 2019, **52**, (28),
670 pp. 106–113
- 671 [39] Morato, M.M., Mendes, P.R.C., Normey-Rico, J.E., Bordons, C.: ‘LPV-MPC fault-tolerant energy management strategy
672 for renewable microgrids’, *International Journal of Electrical Power & Energy Systems*, 2020, **117**, pp. 105644
- 673 [40] Mayne, D.Q., Rawlings, J.B., Rao, C.V., Scolaert, P.O.: ‘Constrained model predictive control: Stability and optimality’,
674 *Automatica*, 2000, **36**, (6), pp. 789–814
- 675 [41] Limón, D., Alvarado, I., Alamo, T., Camacho, E.F.: ‘MPC for tracking piecewise constant references for constrained linear
676 systems’, *Automatica*, 2008, **44**, (9), pp. 2382–2387
- 677 [42] Ferramosca, A., Limon, D., Alvarado, I., Alamo, T., Camacho, E.F.: ‘MPC for tracking of constrained nonlinear systems’.
678 In: Proceedings of the 48th IEEE Conference on Decision and Control held jointly with 28th Chinese Control Conference,
679 2009. pp. 7978–7983
- 680 [43] Cisneros, P.G., Werner, H.: ‘Fast nonlinear MPC for reference tracking subject to nonlinear constraints via quasi-LPV
681 representations’, *IFAC-PapersOnLine*, 2017, **50**, (1), pp. 11601–11606
- 682 [44] Shamma, J.S.: ‘An overview of lpv systems’. In: Control of linear parameter varying systems with applications. Springer,
683 2012. pp. 3–26
- 684 [45] Blanchini, F.: ‘Set invariance in control’, *Automatica*, 1999, **35**, (11), pp. 1747–1767
- 685 [46] Mate, S., Kodamana, H., Bhartiya, S., Nataraj, P.S.V.: ‘A stabilizing sub-optimal model predictive control for quasi-linear
686 parameter varying systems’, *IEEE Control Systems Letters*, 2019,
- 687 [47] Limon, D., Alamo, T., Camacho, E.F.: ‘Enlarging the domain of attraction of MPC controllers’, *Automatica*, 2005, **41**,
688 (4), pp. 629–635

- 689 [48] Tudón.Martínez, J.C., Fergani, S., Sename, O., Martínez, J.J., Morales.Menendez, R., Dugard, L.: ‘Adaptive road profile
690 estimation in semiactive car suspensions’, *IEEE Transactions on Control Systems Technology*, 2015, **23**, (6), pp. 2293–2305
- 691 [49] Cvok, I., Deur, J., Tseng, H.E., Hrovat, D. ‘Comparative performance analysis of active and semi-active suspensions with
692 road preview control’. In: The LAVSD International Symposium on Dynamics of Vehicles on Roads and Tracks. Springer,
693 2019. pp. 1808–1818
- 694 [50] Bumroongsri, P., Kheawhom, S.: ‘An off-line robust MPC algorithm for uncertain polytopic discrete-time systems using
695 polyhedral invariant sets’, *Journal of Process Control*, 2012, **22**, (6), pp. 975–983